R/V Thompson EM302 SAT

University of New Hampshire, Center for Coastal and Ocean Mapping
Jonathan Beaudoin and Val Schmidt
October 15-20, 2010
Version 4 (December 3, 2010)

Table of Contents

Executive Summary

A sea acceptance trial (SAT) was conducted to evaluate the performance of the EM302 multibeam echosounder (MBES) onboard the R/V Thomas G. Thompson in October 2010 off the coast of Washington state. Excellent sea conditions permitted continuous acquisition with all planned survey sites being successfully mapped. It is the intent of this report to document the results of the SAT and to provide recommendations on further improvements that can be made to maximize the performance and accuracy of the system for both bathymetric and acoustic backscatter measurements.

Verification of the configuration of the MBES and all ancillary sensors was done during transit to the deep water patch test calibration site (the same site used for the Thompson's EM300 SAT in 2002) with minor discrepancies being found. These were brought to the attention of the Kongsberg Maritime (KM) personnel who then corrected the configuration in the KM acquisition software (SIS). Patch test operations allowed for the estimation of residual timing and angular misalignments between the MBES and motion reference unit (MRU). Data from the patch test were independently evaluated by the authors and the KM personnel with similar results.

A series of bathymetric surveys were conducted after the patch test over a range of water depths. A deep water survey (1400m-2500m) was conducted using a 5 by 5 survey line grid with survey line directions for survey differing by ninety degrees. Results from the surveys run in different directions confirm the internal consistency of the system and indicate that the MBES and all ancillary systems are being correctly integrated to provide georeferenced soundings. The deep water site was chosen to match the same area mapped by the Thompson during the 2002 EM300 SAT; the 2002 and 2010 grids were statistically consistent within the expected noise level of the system and are a good indication of the absolute accuracy of the system. Backscatter data were acquired over the deep water site as well with results being consistent between the two 2010 surveys, differing in survey direction, and between the 2002 and 2010 surveys. Minor beam pattern artifacts were observed, these were readily removed via standard normalization techniques.

Two shallower water surveys were conducted in ~150 meters of water on the continental shelf and in Puget Sound. Cross lines were acquired during the shelf survey and allow for a quantitative assessment of the system's performance in shallower water. Results were within expected uncertainty levels across the majority of the swath with some minor bottom mistracking issues in the nadir region. Significant beam pattern type anomalies were observed in the transmit sectors immediately adjacent to the nadir region with some discrepancies between the swaths of the dual swath geometry; these are the likely cause of the nadir mistracking issues mentioned earlier. The beam pattern type artifacts are consistent with an incorrect transmitter source level and/or beam steering configuration both of which can be rectified through corrections applied in a configuration file on the sounder.

The shallow survey conducted in Puget Sound attempted to mitigate the nadir mistracking issues by intentional forward steering of the transmitter fan by 6º to 8º. This technique, though successful in minimizing the nadir mistracking, introduced a "hump" type artifact, likely due to bottom tracking algorithms locking on to the transmitter sidelobe response from nadir. Optimization of this technique may yield a configuration that minimizes both of these effects, however, further testing is required. It should be noted that the same backscatter anomalies observed during the shelf survey were also observed during the Puget Sound survey and also throughout the transit data acquired in and out of Puget Sound.

Acoustic noise level measurements were conducted immediately after the deep water survey with the vessel at rest in the water and at a variety of vessel speeds. Results indicate that flow and machinery noise are consistent at speeds below 8kts and only increase slightly (~5dB) at 10 and 12 kts. The low noise level at high speeds and the dual swath capability of the EM302 allow for potentially higher survey speeds as compared to the older EM300 configuration. It should be noted that noise tests in foul weather were not conducted.

The results from all tests and analyses indicate that the EM302 system is performing as expected with minor issues associated with transmit sector configurations affecting bottom tracking performance and quality of acoustic backscatter measurements in the shallow mode of operation. Further testing can be done to address these deficiencies and improve the overall performance of the system.

Introduction

In early October, 2010, the Kongsberg 30kHz EM300 multibeam sonar aboard the R/V Thomas G. Thompson was upgraded to an EM302 system. This upgrade preserved the existing 1ºx1º transducer arrays but incorporated new inboard electronics and software. New capabilities increase the number of soundings per ping from 132 to 432, allow for dual swath transmission in a single ping cycle, and provide linear-frequency-modulated (LFM) pulses for increased signal to noise during deep-water operations. A “Sea Acceptance Test” (SAT) was performed off the Washington coast and is the subject of this cruise report.

EM302 Test Operations

Verification of lever arm and angular offsets in the MRU and MBES

The ship survey positions of the sensors on the vessel were examined and cross checked with the offsets as input to the POS/MV MRU and EM302 MBES. The POS/MV configuration for the "sensor 1" lever arms was found to be consistent with the survey location for the EM302 receiver array (X: 1.825m Y: 1.432m Z: 6.292m)

The POS/MV navigation output for "sensor 1" is the primary navigation that is used by the EM302. The attitude output is configured for "sensor 1" thus the reported heave is that of the receiver array and includes the effects of induced heave. The "sensor 2" offsets in the POS/MV appear to be used for heave correcting the Knudsen 3.5kHz system.

The "auxiliary GPS input" offsets in the POS/MV appear to correspond to an older navigation system that is no longer in use. **It is recommended that these offsets be set to zero to avoid future confusion.**

The EM302 system uses the receiver array as the reference point (sensor 1 in the POS/MV, see above), thus there are no additional navigational corrections to be made for the primary navigation stream in SIS.

The auxiliary navigation feed into the EM302 corresponds to the CNAV system and can be used to georeference the data in the event of a failure in the primary system. As the position reported by the CNAV system is that of the GPS receiver antenna, its position relative to the EM302 reference point must be known in the event that the auxiliary navigation system is to be used. The position for the CNAV antenna relative to the EM302 receiver was calculated from the ship survey and found to be inconsistent with the position recorded in the EM302 configuration.

X: -6.859 (was -6.04)
Y: 1.060 (was 1.37)
Z: -30.868 (was correct)

These have been corrected in the EM302 system.

The position of the transmitter array was calculated from the ship survey and found to be slightly inconsistent with the position recorded in the EM302 configuration.

X: 1.95 (was correct)
Y: 0.61 (was correct)
Z: 0.01 (was 0.13)

The z value has been corrected in the EM302 system.

The water line z value of -5.85 cannot be confirmed with the survey data. **It is recommended that this value be confirmed with dockside observations upon return.**

The installation angles of the EM302 transmitter and receiver were double checked against the ship survey results. The sign of the transmit pitch angle was found to be incorrect in the EM302 configuration (was 0.14, should be -0.14). This value was corrected in the EM302 configuration.

Angular offsets for the IMU were found in the EM302 configuration files (which were based on the EM300 configuration files prior to it being disassembled); no record of these offsets was found in the ship survey documentation. Since these offsets are small, there is little harm in leaving them in place as the patch test calibration procedure will correct for their effects if they are indeed incorrect.

Patch Test

A patch test was conducted on October 17th in the same area as the 2002 EM300 SAT in water depths ranging from 1400m to 1900m (approximate location 47°36.7'N 126°2.5'W). The angular and lever arm offsets ascertained from the 2002 survey were used as initial offsets for the MBES, GPS and MRU. Results of the patch test are summarized below.

Navigation time delay: 0.0 seconds
Roll correction: -0.05º
Pitch correction: 0.00º
Yaw correction: -0.20º

The above values are corrections that must be added to the existing MRU offsets. The final MRU angular offsets are summarized below:

Navigation time delay: 0.0 seconds

Total roll offset: -0.31 + (-0.04) = -0.35º
Total pitch offset: 0.00 + 0.00 = 0.00º
Total yaw offset: 0.00 + (-0.20) = -0.20º

After the SAT survey (see next section), it was realized that the MRU yaw offset was incorrectly entered in SIS as -0.02º (instead of -0.20º). This was brought to the attention of the Kongsberg technicians who then corrected the system installation parameters.

Deep Survey

A 5x5 line grid survey was conducted after the patch test immediately to the southwest of the patch test area in water depths ranging from 1400m to 2500m (in the same area as the EM300 SAT survey, see Figure 1).

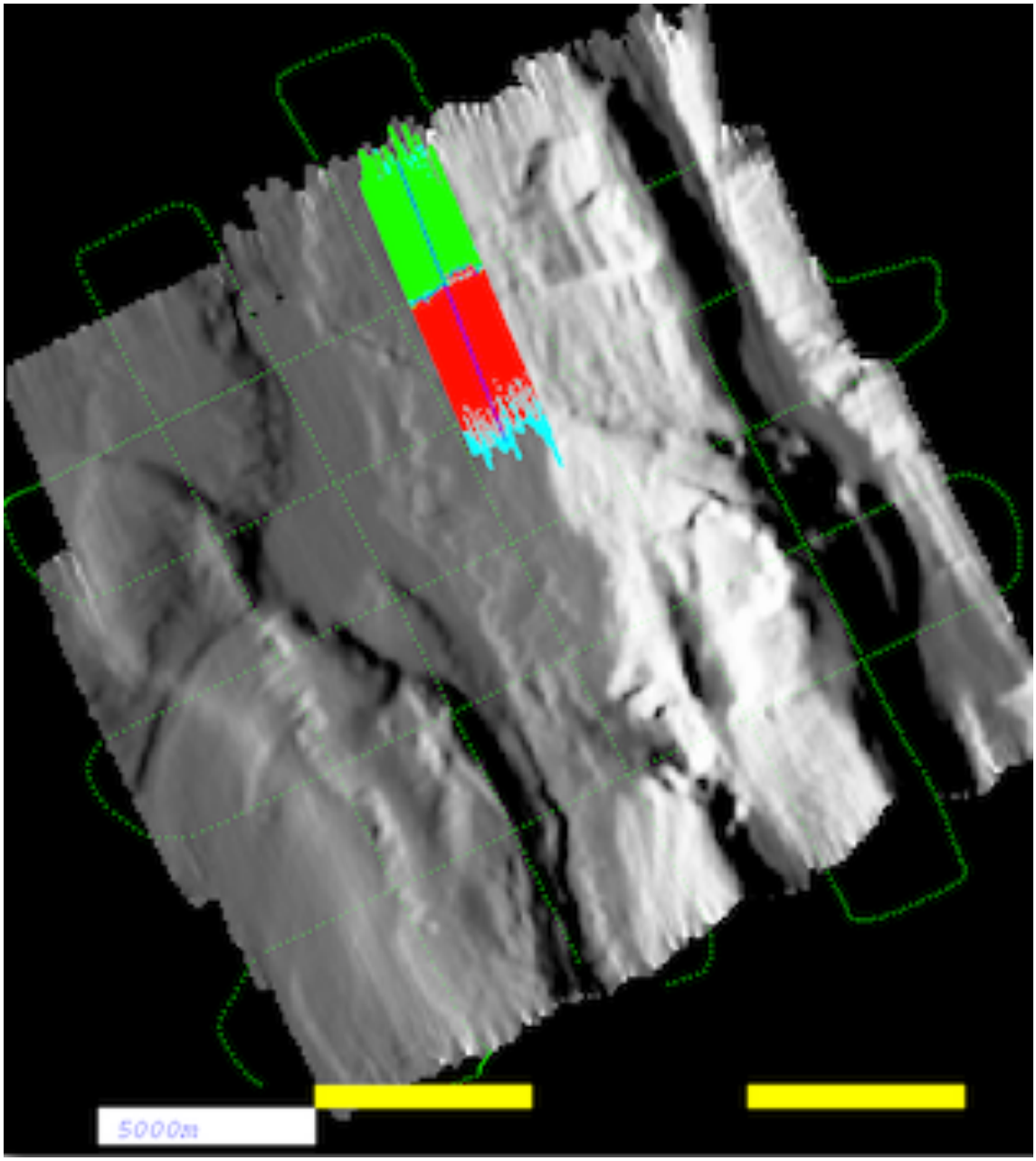

Figure 1. SAT Main survey with grid lines superimposed. Swath coverage for 100 pings is shown as red/green dots (cyan dots are filtered outlier detections).

The survey took ~16 hours to complete at a speed of 8kts with the sounder configured to run in "Deep" mode with mixed CW/FM waveforms. The angular sector was constrained to +/- 65º, allowing for greater than 100% overlap between survey lines giving greater than 200% coverage in most cases. Pitch/yaw stabilization and dynamic dual swath modes of operation were activated in order to maintain consistent sounding density in the along-track and across-track directions throughout the survey area. Waveform characteristics varied with sector and swath number (of the dual swath pair), these are summarized below.

Ping 1 of dual swath

1: Signal Length: 0.0400s, Center Frequency: 28.1 kHz, Waveform: FM
2: Signal Length: 0.0250s, Center Frequency: 26.5 kHz, Waveform: FM
3: Signal Length: 0.0075s, Center Frequency: 31.3 kHz, Waveform: CW
4: Signal Length: 0.0075s, Center Frequency: 29.7 kHz, Waveform: CW
5: Signal Length: 0.0075s, Center Frequency: 31.7 kHz, Waveform: CW
6: Signal Length: 0.0075s, Center Frequency: 30.1 kHz, Waveform: CW
7: Signal Length: 0.0250s, Center Frequency: 28.5 kHz, Waveform: FM
8: Signal Length: 0.0400s, Center Frequency: 26.9 kHz, Waveform: FM

Ping 2 of dual swath

1: Signal Length: 0.0400s, Center Frequency: 28.9 kHz, Waveform: FM
2: Signal Length: 0.0250s, Center Frequency: 27.3 kHz, Waveform: FM
3: Signal Length: 0.0075s, Center Frequency: 32.1 kHz, Waveform: CW
4: Signal Length: 0.0075s, Center Frequency: 30.5 kHz, Waveform: CW
5: Signal Length: 0.0075s, Center Frequency: 32.5 kHz, Waveform: CW
6: Signal Length: 0.0075s, Center Frequency: 30.9 kHz, Waveform: CW
7: Signal Length: 0.0250s, Center Frequency: 29.3 kHz, Waveform: FM
8: Signal Length: 0.0400s, Center Frequency: 27.7 kHz, Waveform: FM

Bathymetry

MBES data were converted into OMG format and visually inspected for outliers in order to remove them prior to gridding. Soundings were georeferenced using the primary navigation system position and heading records (POS/MV) and tidally reduced using a global tidal model. Grid files were created at 100m resolution for the main lines and cross lines using the standard an inverse-distance weighting approach based on a linear beam angle weighting and a projected beam footprint for the radius of influence. The grids were differenced to estimate the internal consistency of the EM302 system as a whole, including all ancillary sensors and the integration thereof. Color coded depth and depth difference images are shown below in Figures 2 and 3.

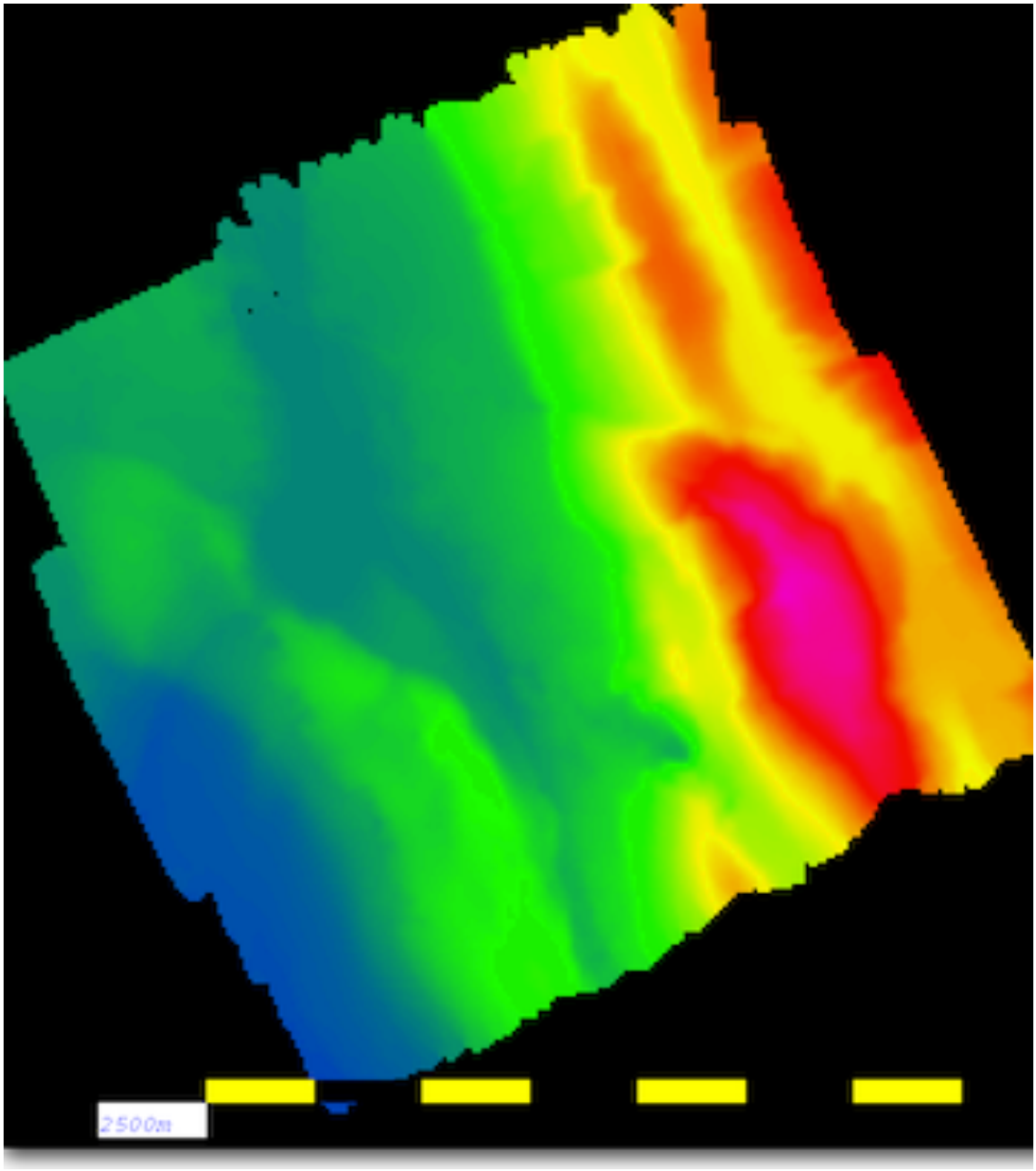

Figure 2. SAT survey area, depth range runs from 2,550m (blue) to 1,200m (magenta).

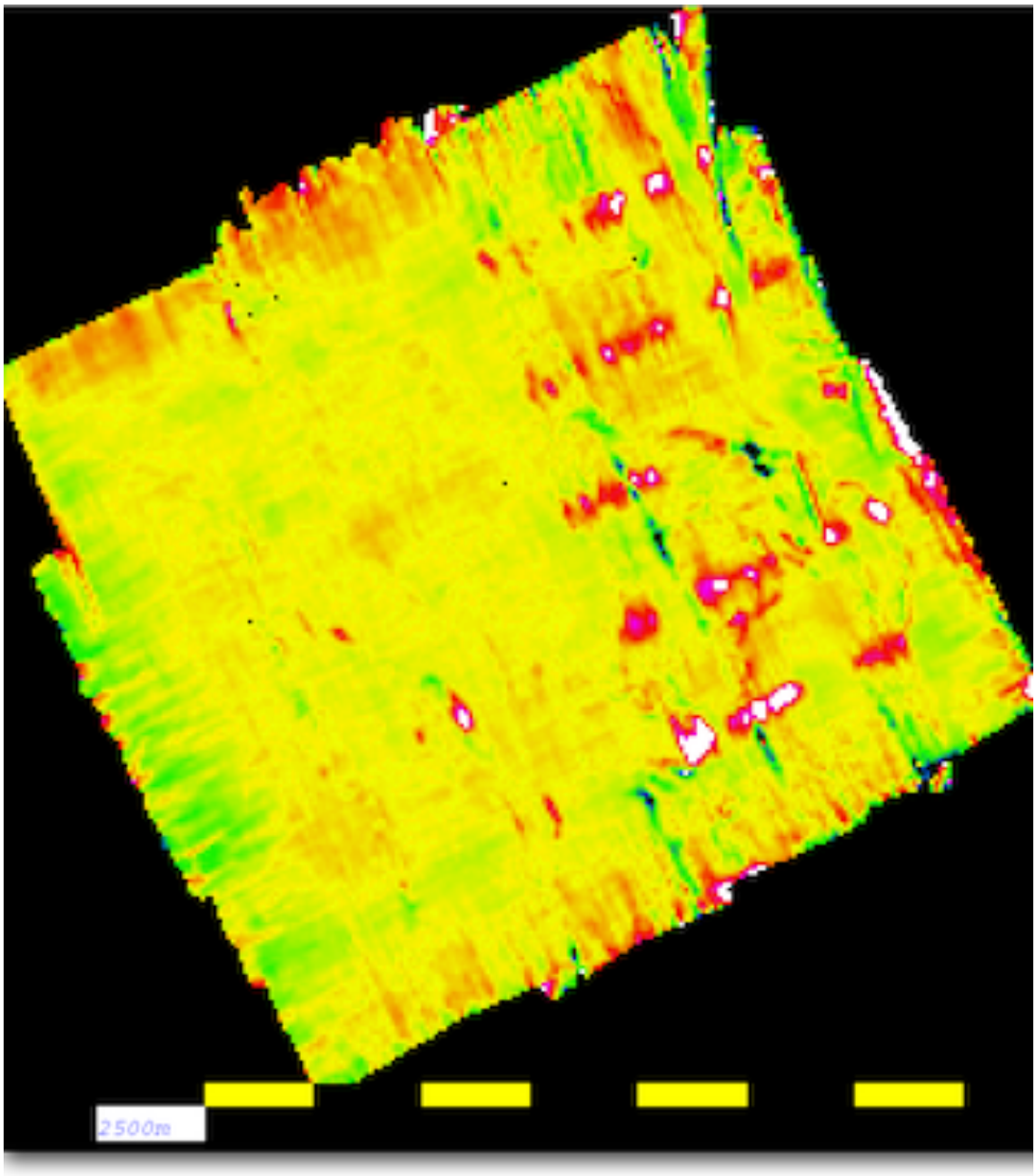

Figure 3. Depth difference between EM302 main line survey and cross line survey. Color coding for differences runs from -15m (blue) to +15m (magenta).

Results were acceptable, despite the incorrect MRU yaw offset: the mean difference between the two gridded surfaces was 0.01%w.d. +/- 0.39%w.d. at the 95%c.l., this is equivalent to ~0.2m +/- 7.8m @ 95% in 2000m of water. The same mainline/crossline comparison procedure was followed for the EM300 data set from 2002 to provide a benchmark against which the EM302 results could be compared. The mean difference between the EM300 main line and cross line grid was 0.01%w.d. +/- 0.48%w.d. @ 95%c.l. The EM302 results are consistent with the EM300 SAT results obtained in 2002 with a slight improvement in overall uncertainty of 0.1%w.d. @ 95%c.l..

The main line grids were compared between the EM300 and EM302 systems and were also found to be consistent with a mean bias of 0.015%w.d. +/- 0.45%w.d. @ 95%c.l. The same was repeated for the cross line grids for each system with a mean bias of 0.01%w.d. +/- 0.44%w.d. @ 95%c.l.

The results are summarized below.

EM302, main line grid vs. cross line grid: 0.01%w.d. +/- 0.39%w.d. @ 95%c.l.
EM300, main line grid vs. cross line grid: 0.01%w.d. +/- 0.48%w.d. @ 95%c.l.
EM300 vs. EM302, main line grids: 0.015%w.d. +/- 0.45%w.d. @ 95%c.l.
EM300 vs. EM302, cross line grids: 0.01%w.d. +/- 0.44%w.d. @ 95%c.l.

The cumulative probability distribution of a single main-line/cross-line intersection is shown below in Figure 4.

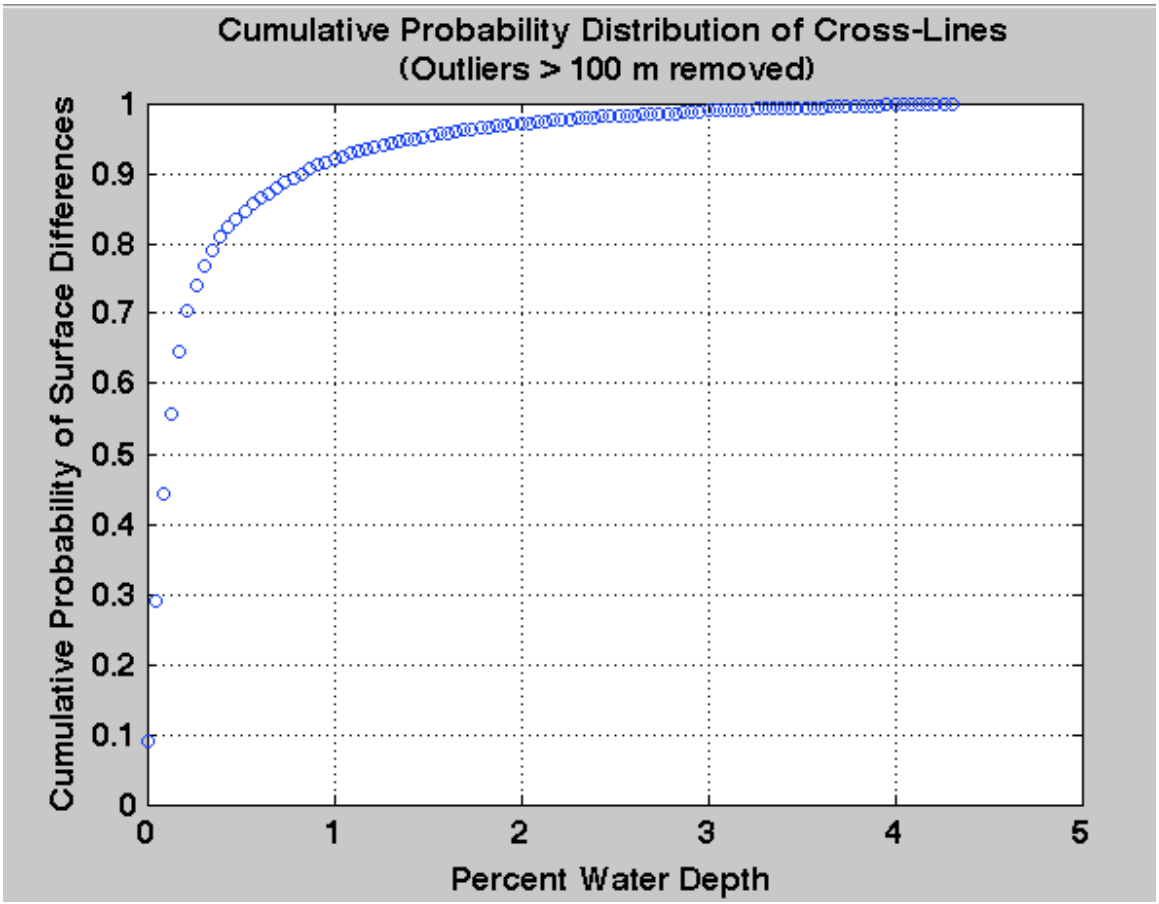

Figure 4. Cumulative probability distribution of differences in depths measured over cross-lines after gross outlier removal. The water depth was approximately 2300 m. The 1-sigma difference is at the 0.2 % of water depth level and is in agreement with the EM302 sonar description.

Beam/sector statistics were computed for the westernmost line (0010_20101018_115800) of the set of cross lines and are shown in Figure 5. Overall bias across the swath is consistent with a minor refraction artifact. Uncertainty across the swath is less than 0.2% (1-sigma) and is consistent with the grid differencing findings above. The higher

uncertainties at the outermost edges is likely due to the increased effects of orientation (roll) and refraction uncertainty. The local maximum of uncertainty in the nadir region is curious and warrants further investigation. It should be noted that the high degree of bathymetric variability in the region is not conducive to estimation of system accuracy; a flat seafloor is much more useful for estimating the total combined uncertainty of the mapping system.

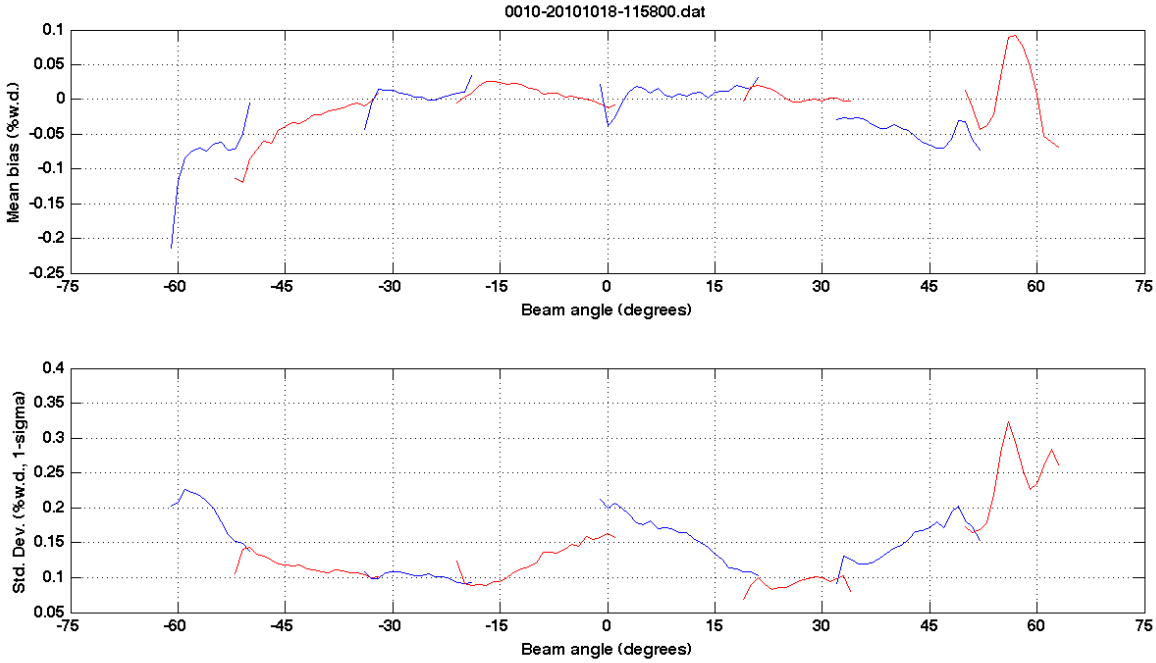

Figure 5. Depth difference statistics compiled by beam angle and color coded by transmit sector.

Backscatter

Backscatter mosaics were prepared for the main and cross line surveys and differenced in order to estimate the repeatability of the backscatter measurements. The backscatter data in raw format are biased by a combination of transmit sector beam pattern, seafloor angular response and an imperfect real-time TVG that appears to overcompensate for seafloor angular response at nadir. A backscatter mosaic of the raw data was prepared for the main survey lines and is shown in Figure 6. The combined effect of the three sources of backscatter bias can be removed through a normalization procedure in which the mean response is calculated by beam angle and is then inverted to remove the effect, resulting in the normalized image in Figure 7. Note the intermittent low backscatter artifacts in the nadir region of the swath in areas of high topography; these cannot be removed by the normalization procedure.

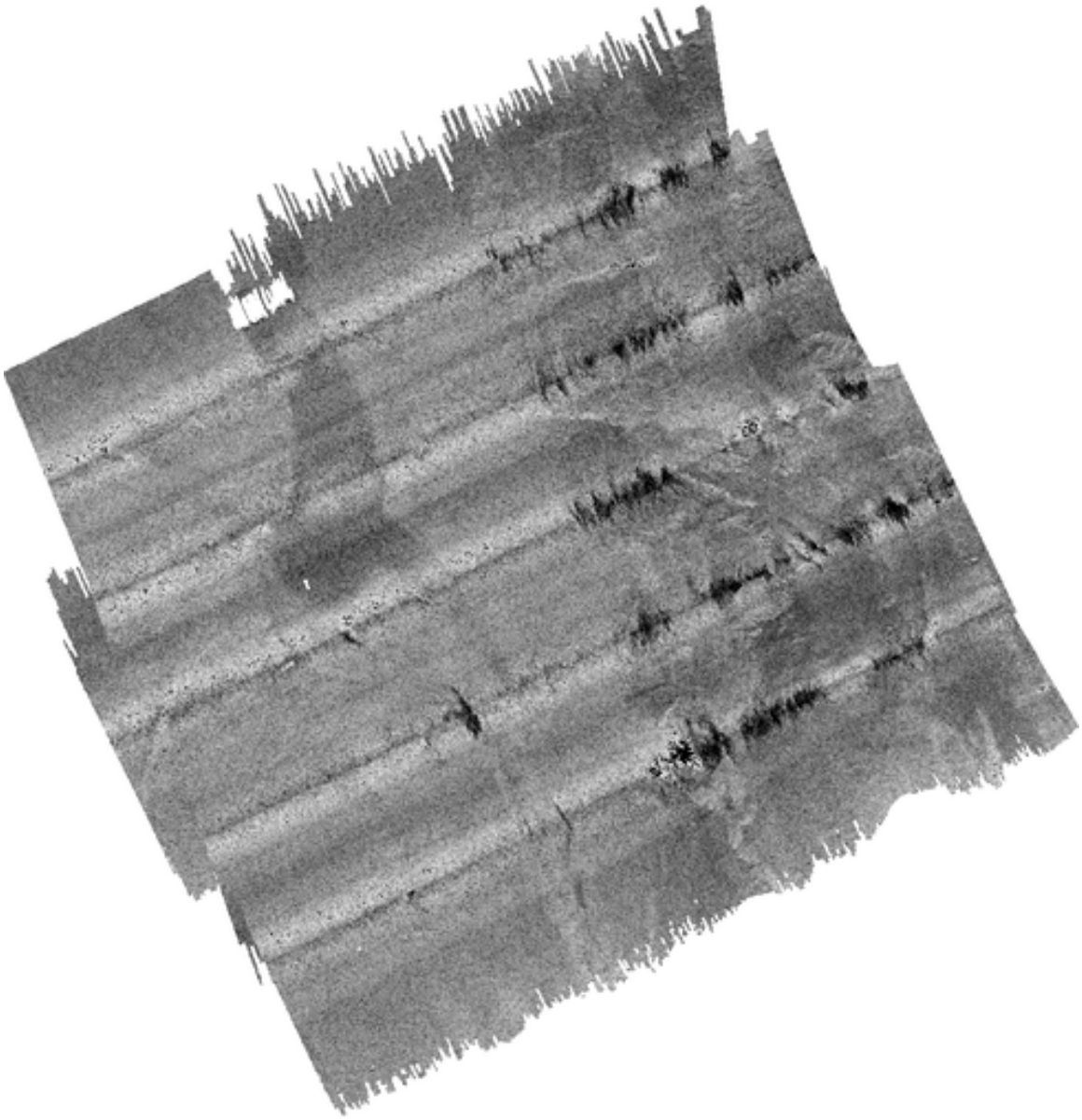

Figure 6. Main survey raw backscatter, backscatter ranges from -40dB (black) to -5dB (white).

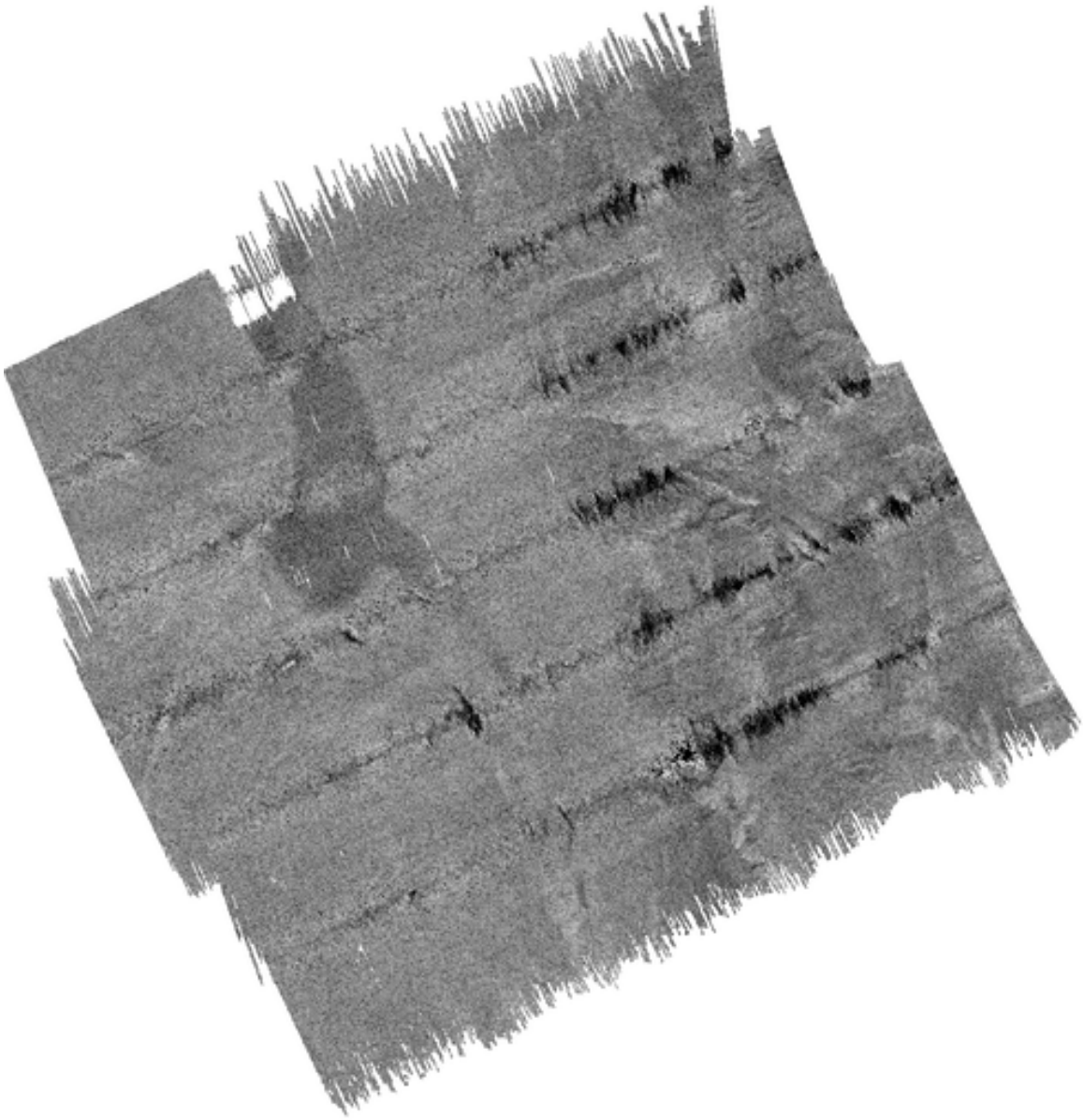

Figure 7. Normalized main line survey backscatter mosaic (-40dB to -5dB, black to white).

Differencing between the normalized main line and cross line mosaics yields a mean difference of -0.6dB +/- 14.8dB @ 95%c.l. It should be noted that the backscatter values in a seemingly homogeneous patch of seafloor (for example, the lower left corner of the survey area) have a 2-sigma standard deviation of ~10dB and that the standard deviation of the difference between the two data sets is simply the quadratic sum of the 10 dB noise level inherent in both mosaics.

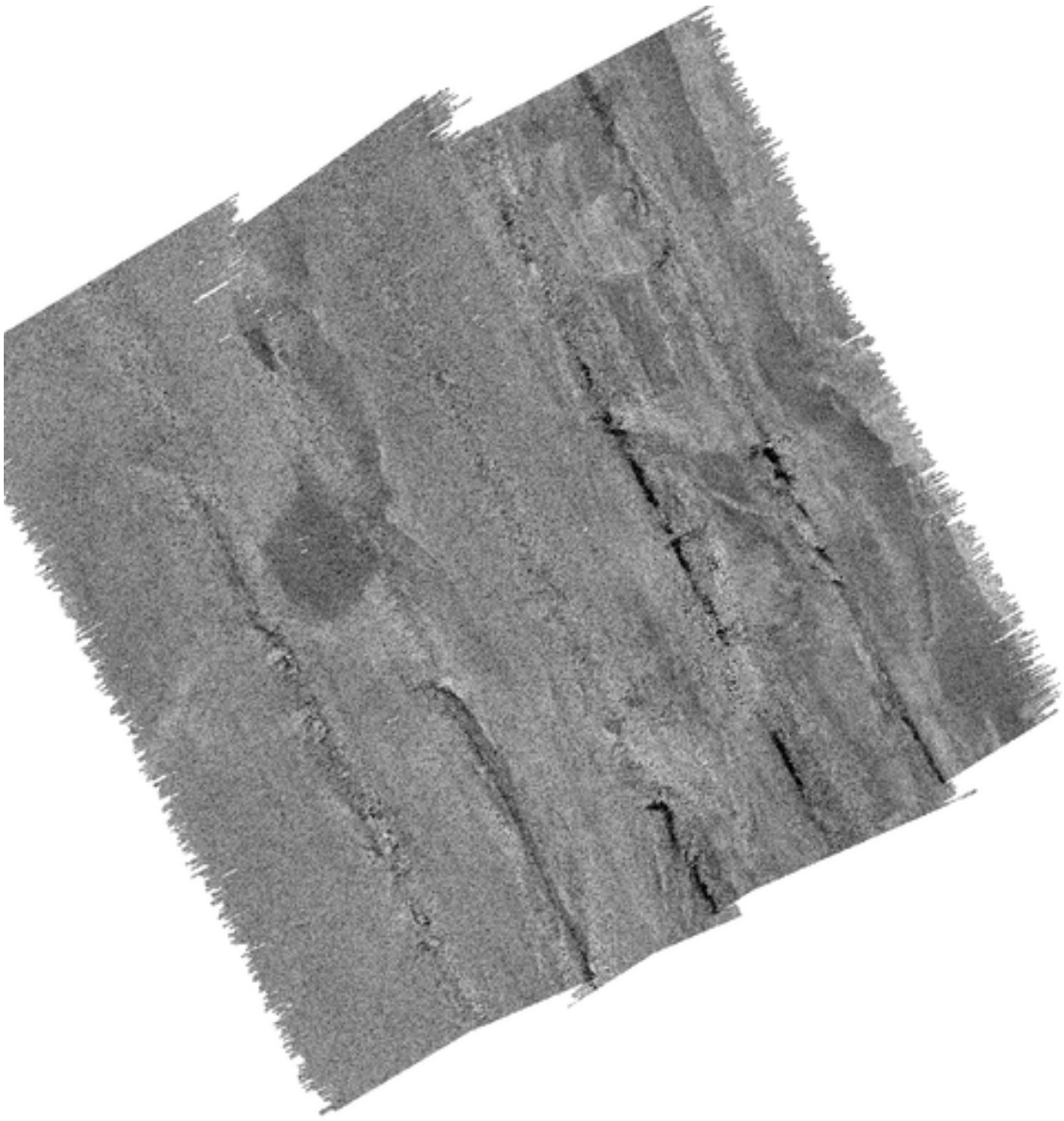

Figure 8. Normalized cross line survey backscatter mosaic (-40dB to -5dB, black to white).

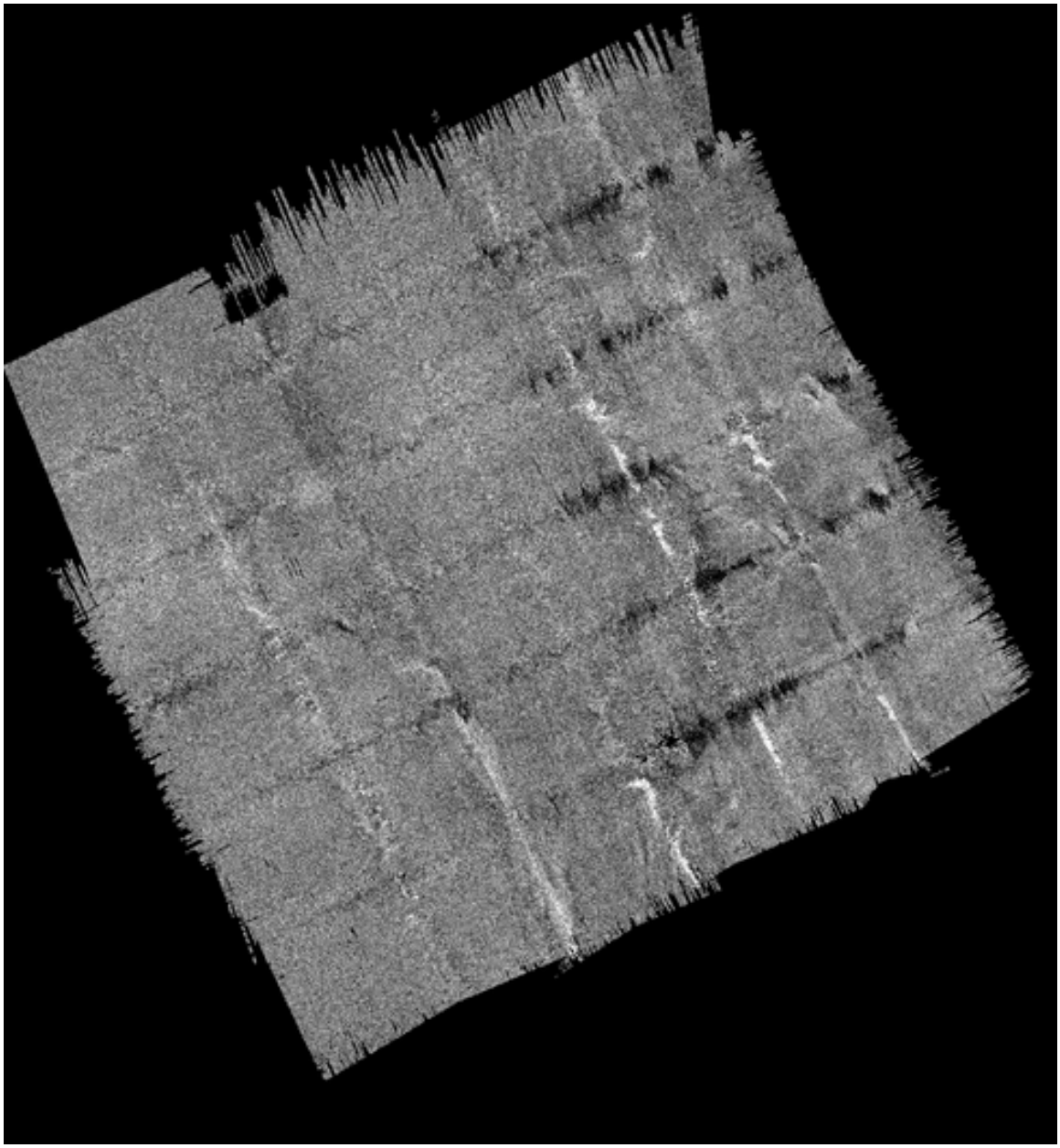

Figure 9. Difference map between main line and cross line backscatter mosaics. Differences span 30dB, from -15dB (black) to +15dB (white).

Beam/sector backscatter difference statistics were computed for the same westernmost line as used in the bathymetric repeatability analysis. The mean differences capture the combined effect of the three sources of bias mentioned earlier, i.e. transmitter beam pattern (by sector), angular response of the seafloor and the failure of the real-time TVG curve to adequately estimate the effect of angular response, especially in areas of high topography. These curves should thus not be globally used for data normalization as they will only be applicable for the mode of operation used during the SAT survey. The standard deviation about the mean bias is consistent across the swath and is also consistent with the differencing uncertainty observed in the overall difference mosaic earlier (+/-7dB scaled to 2-sigma is +/-14dB). The obvious exception to this observation

is the nadir region, a region in the swath imaging geometry that is particularly troublesome for backscatter measurement due to the highly specular nature of the acoustic reflections. This source of uncertainty is further compounded by the odd behavior of the Kongsberg real-time TVG in the nadir region which often overcompensates for the specular reflections at nadir, thus the higher uncertainties observed at nadir are not surprising.

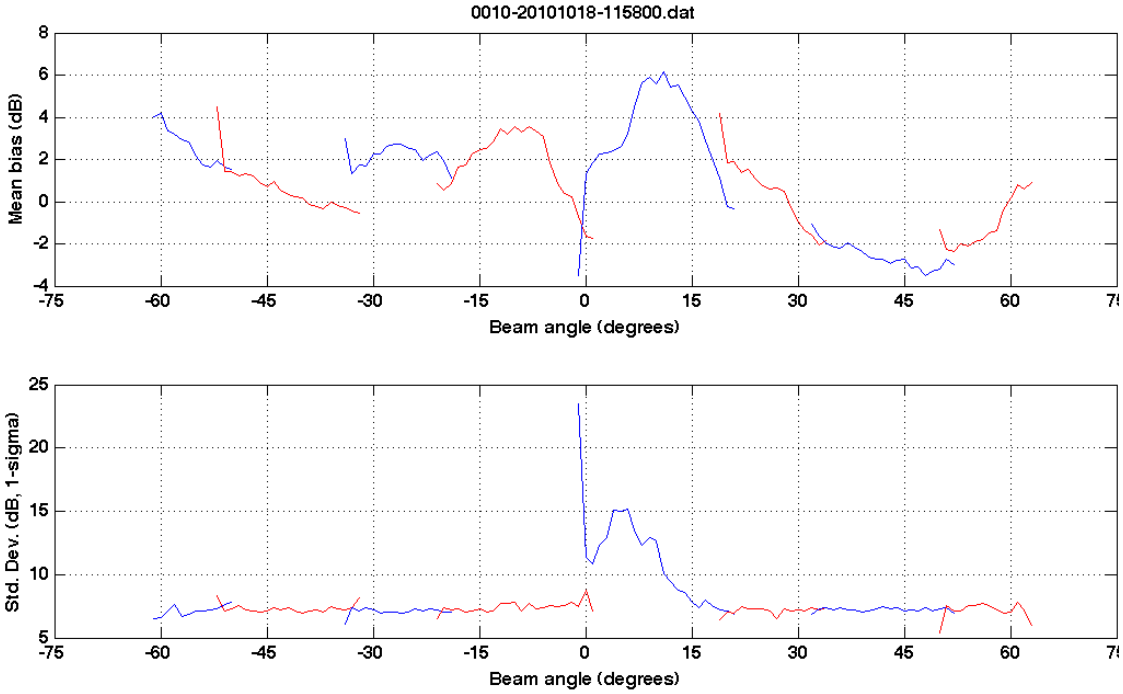

Figure 10. Backscatter difference statistics compiled by beam angle and color coded by transmit sector.

Shallow Survey

A shallow water survey was performed on the continental shelf in water depths ranging from 130 to 160m located at 46º52'N/124º44'W over an area approximately 13km x 13km in size (see Figure 11). Pockmark features were located in the survey area and were the primary focus of the survey. Water column data were logged for the express purpose of imaging gas venting over the pockmarks. A total of five main survey lines were planned, running in the NW/SE direction, two cross lines were collected in the vicinity of the pockmark features. An XBT profile was collected immediately prior to the survey and a second profile was acquired prior to running cross lines.

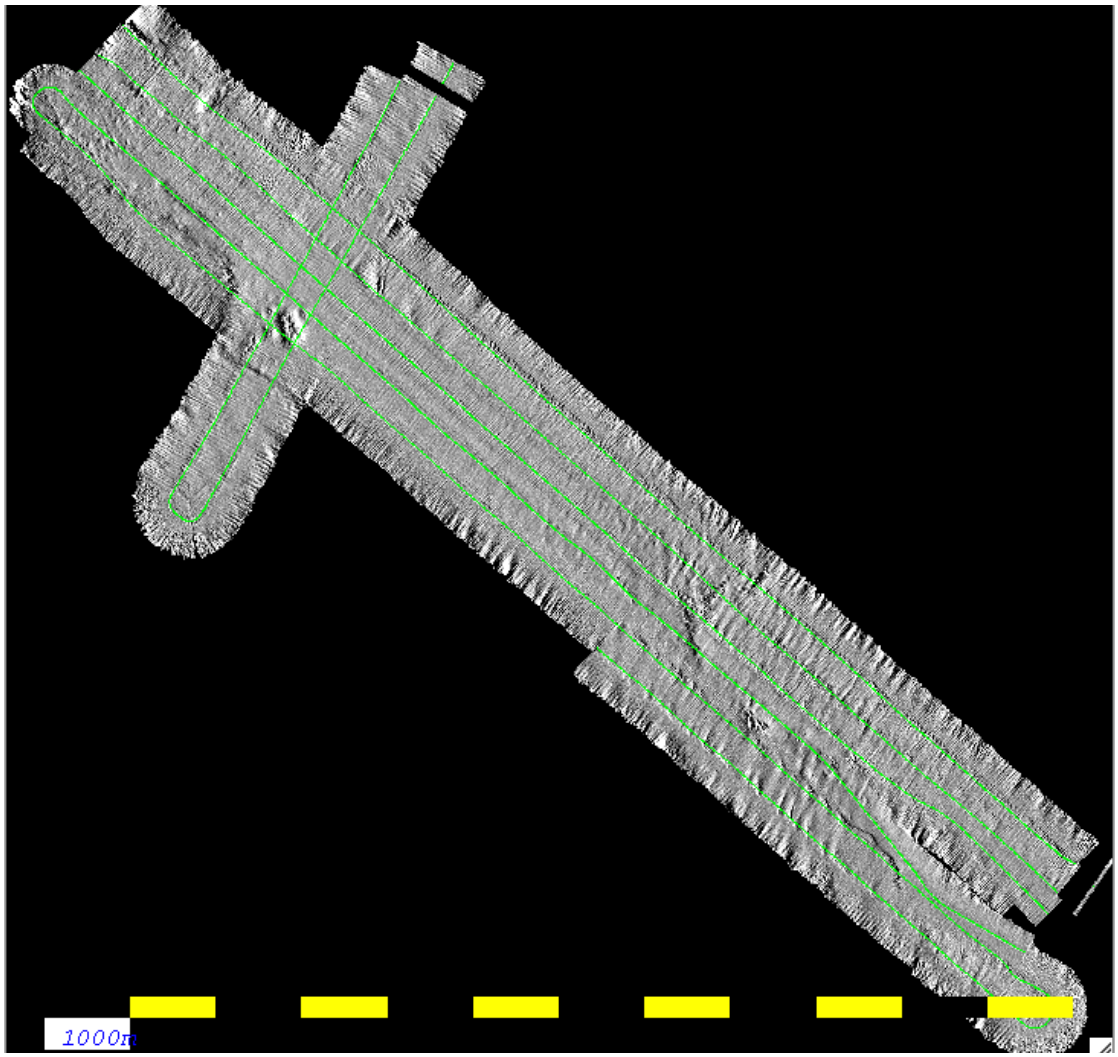

Figure 11. Overview map of shallow site survey.

Significant heave like artifacts were noticed on three of the main lines (long period with magnitude ~0.5m, 50-100m wavelength). The artifacts were preferentially associated with northwesterly running survey lines and were significantly attenuated on southeasterly running lines, see figures 12 and 13. This is consistent with long period heave residuals associated with the apparent Doppler shift in short period vertical motion associated with running with and against the swell. After the survey, it was found that the POS/MV heave filter length was set at 18 seconds; it is recommended that this be shortened to improve performance in these scenarios. An exact filter length will depend on the surface wave spectra and could vary from survey to survey thus further investigations should be made to determine an appropriate setting.

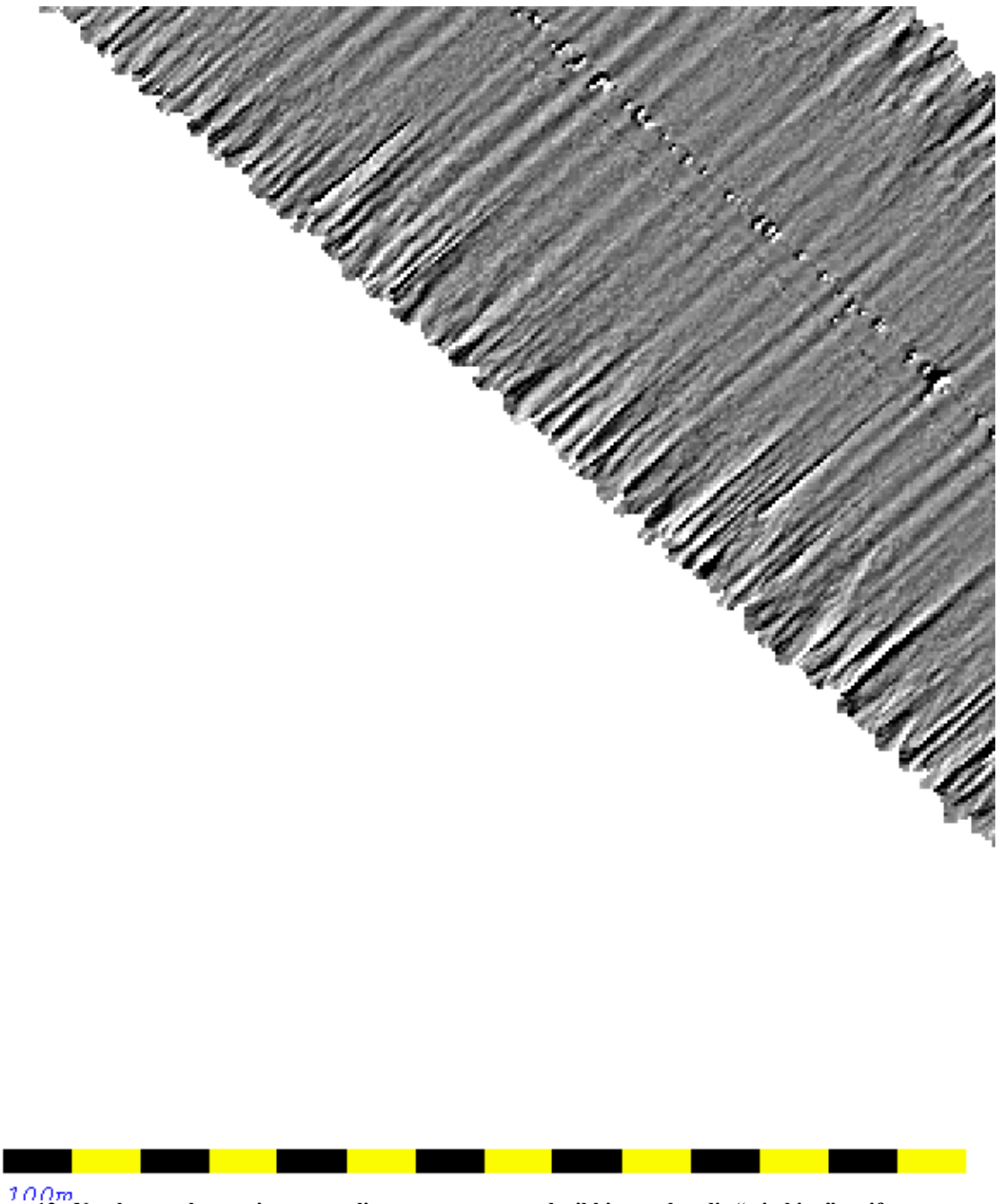

Figure 12. Northwesterly running survey line, note across-track ribbing and nadir "stitching" artifacts.

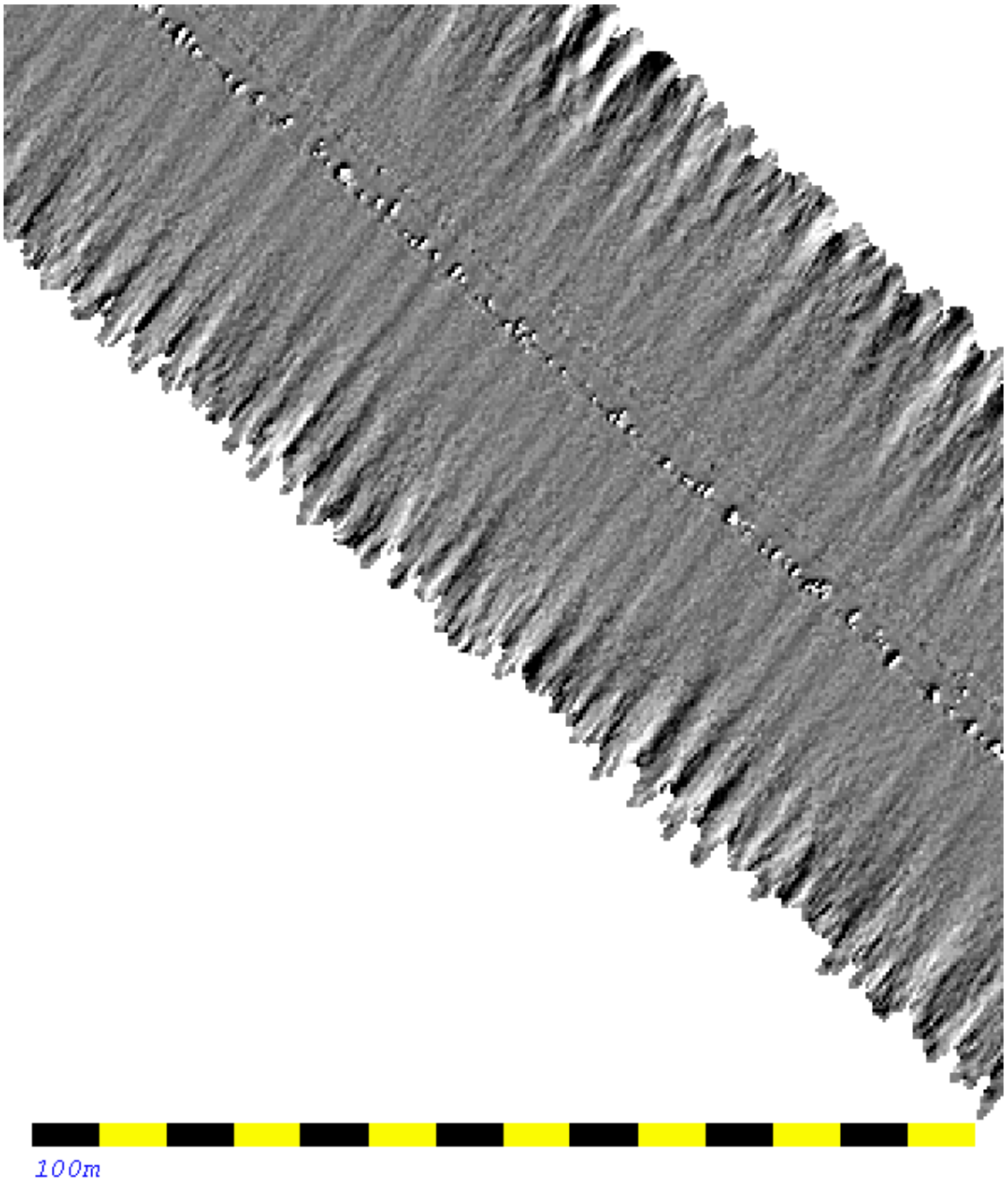

Figure 13. Southeasterly running survey line, note muted across-track ribbing compared to previous line. Outer beam artifacts are consistent with internal wave effects on ray bending corrections.

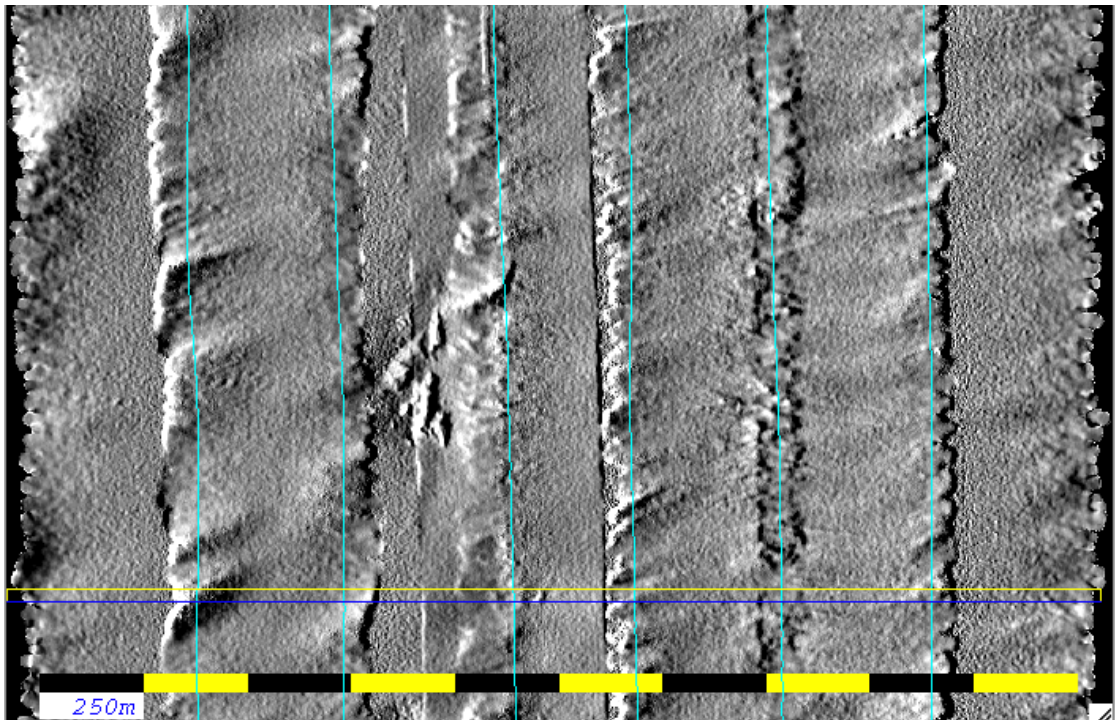

Figure 14. Sun-illuminated topography of the southeastern section of the shallow survey area. Only the small outcrop feature just slightly left of center is real, all other features are refraction type artifacts likely due to internal wave activity perturbing the acoustic ray path. The long rectangular area highlighted in yellow is shown as a cross-section of soundings in Figure 15.

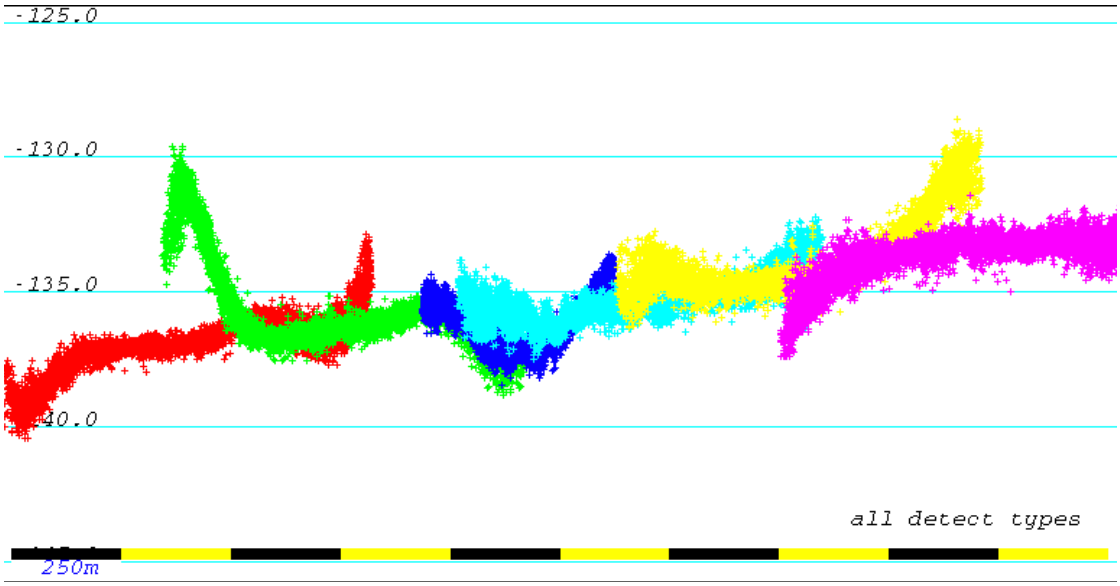

Figure 15. Cross-section of soundings from the image of Figure 14. Inconsistencies in areas of overlap are due to refraction type artifacts commonly associated with internal wave perturbations of the thermocline (note the asymmetric refraction artifact on the green soundings).

Refraction type artifacts were the primary source of system inaccuracy as shown in Figures 14 and 15. The artifacts are indicative of a highly variable water mass and are consistent with artifacts due to internal wave perturbations of the thermocline (Hamilton,

2010). Internal waves have been observed along the Oregon coast (Moum, 2003) and it is likely a safe assumption that the same triggering mechanism and physical conditions exist in the vicinity of the shallow survey due to (a) the proximity to the shelf break and (b) the strong temperature stratification of the water mass, as evidenced by the XBT measurement prior to the survey (see Figure 16). Further examination of the ADCP data might provide more evidence of internal wave activity.

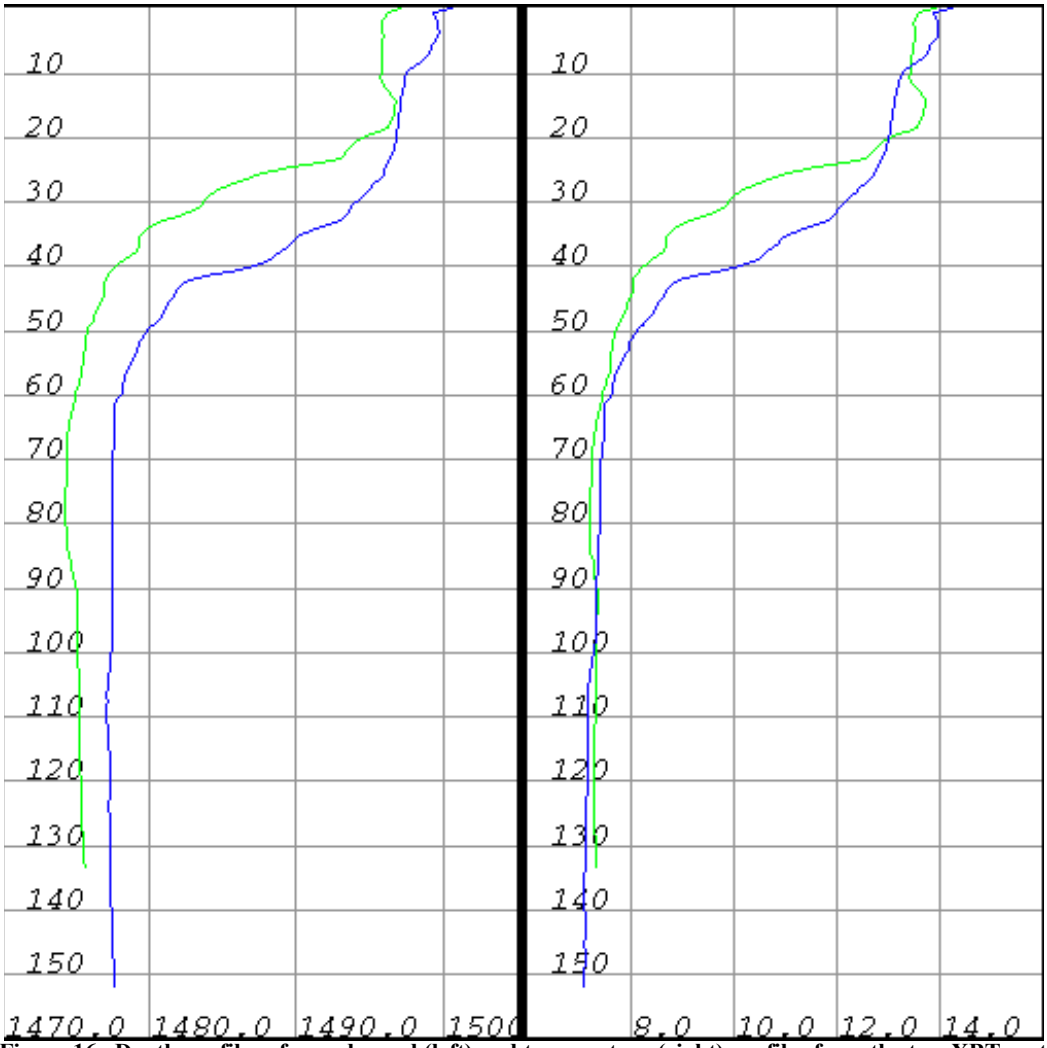

Figure 16. Depth profiles of sound speed (left) and temperature (right) profiles from the two XBT casts acquired during the survey. Note the pronounced sound speed/temperature gradient between depths of 20m and 40m. Units for depth, sound speed and temperature are meters, meters/sec and °C, respectively.

The two cross lines allow for estimation of the EM302 mapping system's internal consistency in continental shelf water depths, however, the presence of significant refraction and heave artifacts limited the cross-line analysis to two of the main lines and to very limited angular sectors thereof. A bathymetric grid of the two main lines were prepared with a angular sector constrained to +/-45º to limit the comparison of the cross line data to main line data of reasonable accuracy. Beam-by-beam statistics are shown in Figure 17 and indicate that the system has acceptable internal consistency within a ~+/-

60º swath angle beyond which refraction based artifacts dominate the systems total propagated uncertainty. It should be noted that, by chance, the cross-line data were not as severely affected by the refraction type artifacts observed elsewhere in the survey area thus these results could have been much worse. In areas of more reasonable water mass conditions it would be expected that improved accuracy would extend to larger angles. The peak features in mean bias and standard deviation centered about 0º are associated with one of the two swaths in the dual swath pair geometry (see the "stitching" artifact at the track center in figures 12 and 13). These soundings would normally be flagged as outliers during post-processing QC procedures, however, it would be preferable if inter-sector filtering could be performed in real-time as the post-processing filtering can be labor intensive.

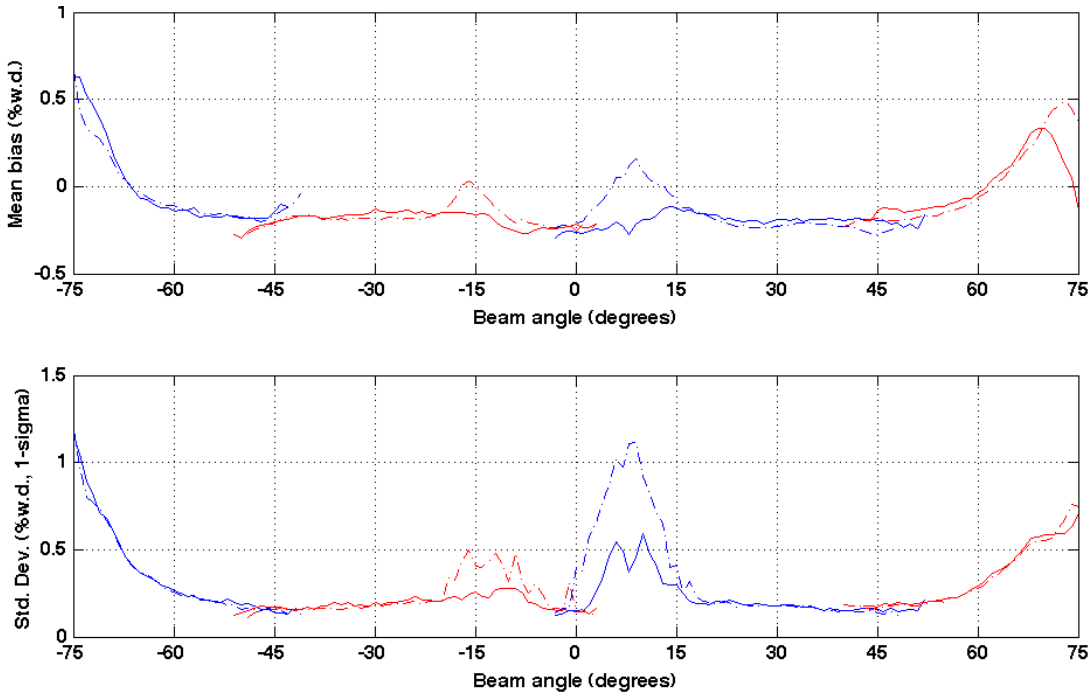

Figure 17. Depth difference statistics compiled by beam angle and color coded by transmit sector. Dashed/solid lines are associated with the ping sequence of the dual swath ping cycle. Note that the artifacts centered about 0º are associated with only 1 ping of the dual swath geometry and is consistent with transmitter sidelobe interference. The overall mean bias of ~0.2% could be explained by (a) a residual refraction artifact and (b) an incorrect tidal reduction (the survey lines analyzed here were collected over a 5 hour time interval, all soundings were refraction corrected with a single XBT profile collected prior to the survey).

A similar analysis was performed on the backscatter data to assess the system's internal consistency in terms of measuring the seabed's acoustic backscattering strength. A mosaic of the raw backscatter data is shown in Figure 18, note the dominant beam pattern type artifacts throughout the survey area.

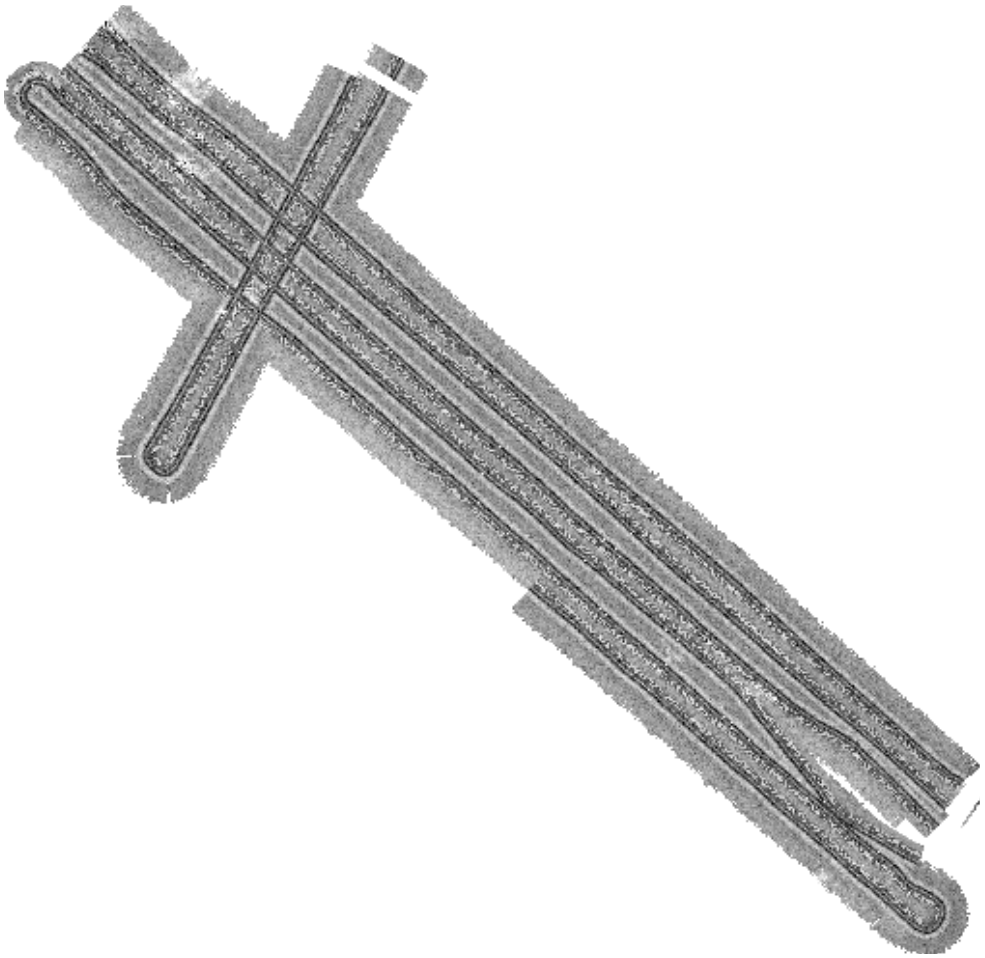

Figure 18. Backscatter mosaic of main and cross lines. Data are "raw" in that no radiometric signal normalization or correction has been applied. Prominent beam pattern type artifacts dominate throughout.

Examining waterfall displays of the backscatter beam values indicates that the beam pattern type artifact is asymmetric about the array normal and also varies by ping sequence in the multi-swath ping cycle, see Figure 19 and 20.

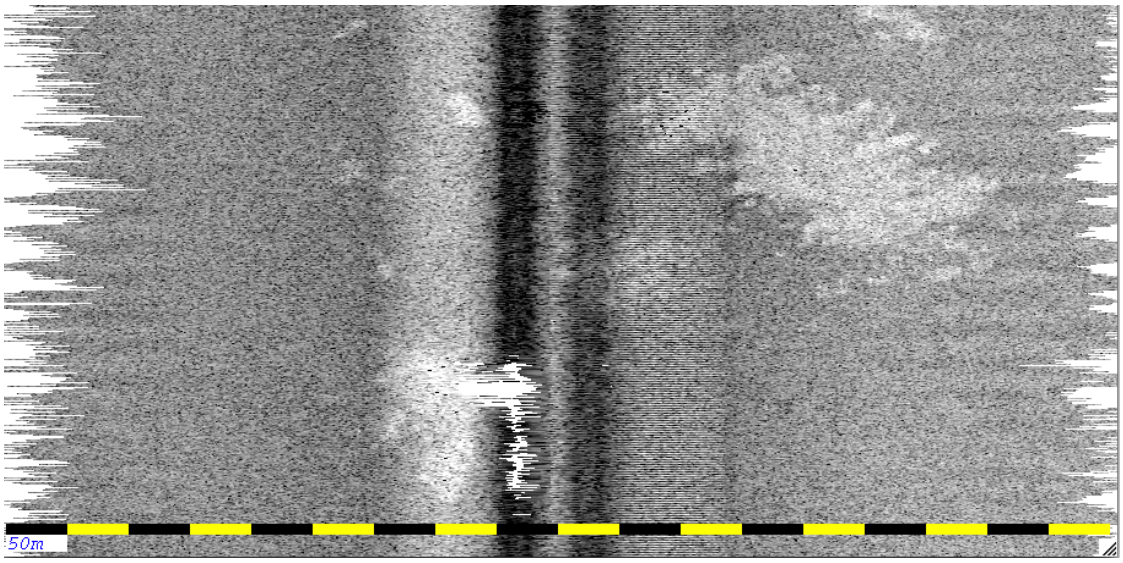

Figure 19. Beam backscatter in a waterfall type display. The vertical axis corresponds to ping number increasing downward. Across-track distance corresponds to the horizontal direction (scale only truly applies in the across-track direction). Note the discrepancy between beam pattern artifacts on either side of nadir.

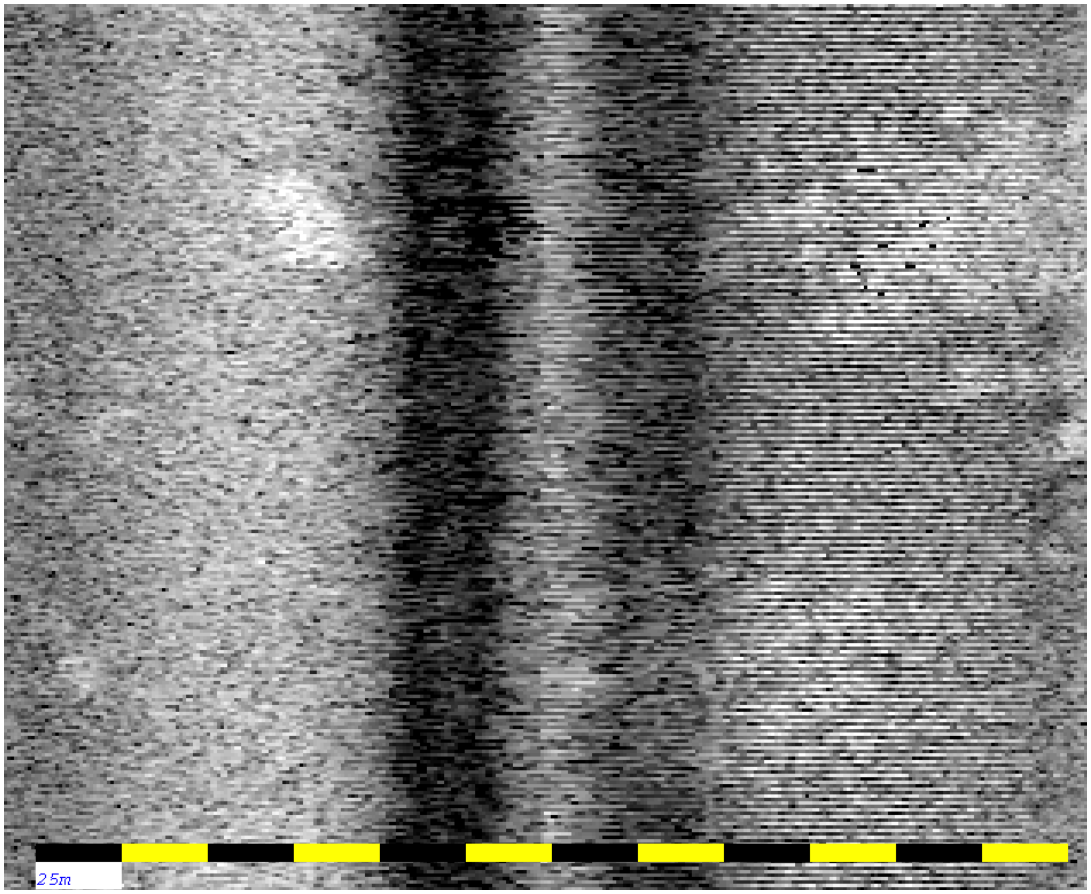

Figure 20. Zoom in of upper central region of Figure 19 showing ping-by-ping differences in the port side data (right of center).

Beam-by-beam statistics were compiled using the cross lines. A smaller mosaic was prepared using the outermost sectors of two of the main line in order to remove the inner portion affected by the beam pattern artifacts, see Figure 21.

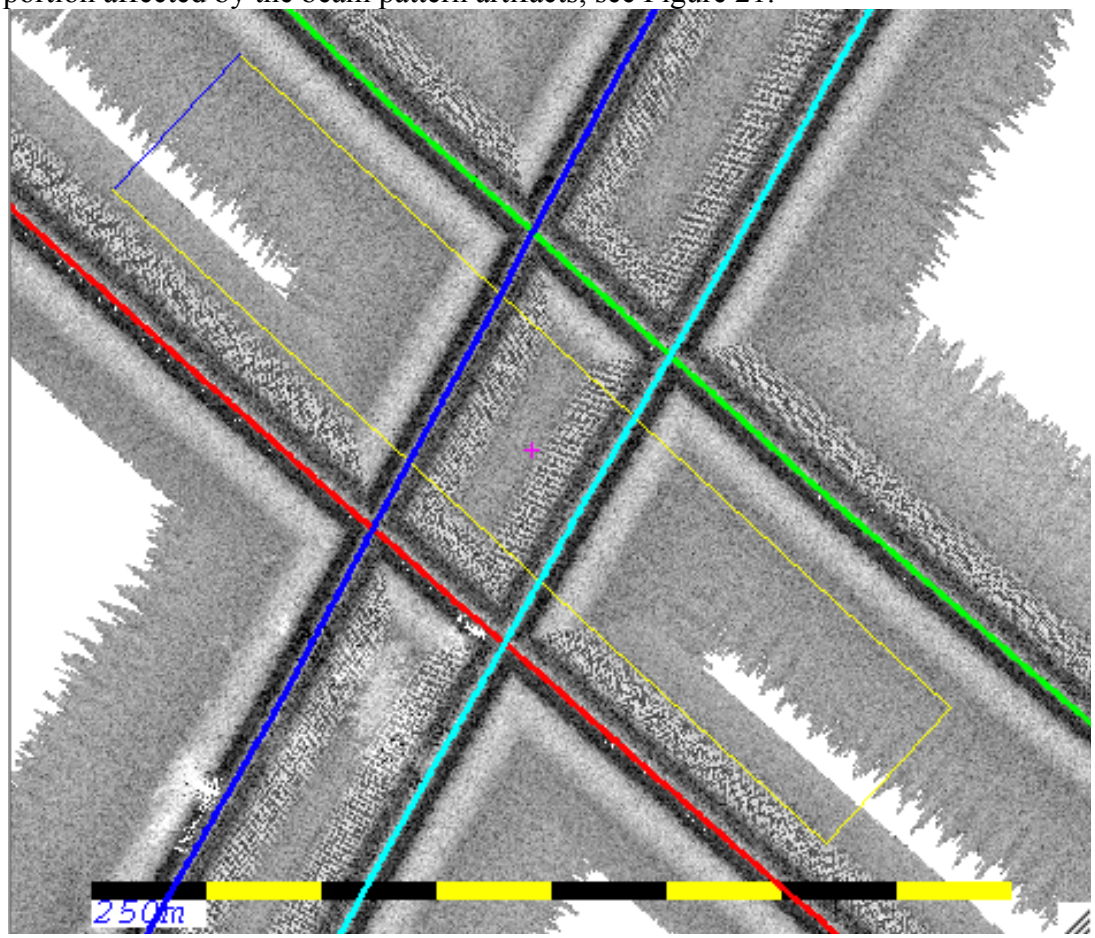

Figure 21. Overlap area used in backscatter beam statistic compilation. The yellow rectangle indicates the overlap area used in the analysis, a mosaic was created from the NW/SE main lines (red and green) in this area against which the NE/SW lines (blue and cyan) were compared.

Beam statistics are shown in Figure 22 and reflect what is easily observable in the backscatter images presented thus far: the sectors neighboring the nadir region suffer from pronounced beam pattern artifacts and there is a significant difference between the ping sequenced sectors on the port side in the multi-swath ping cycle. The beam pattern type artifacts results from the interplay of three effects: (1) transmitter/receiver beam patterns, (2) the seafloor's varying angular response with grazing angle, and (3) the Kongsberg real-time TVG that attempts to compensate for (2). It is interesting to note that these effects are particularly pronounced in the shallow water survey but are largely absent from the calibration survey conducted in much deeper water (1400m to 2500m). This indicates that the problem is not likely due to transmitter beam patterns associated with the transmitter transducer hardware and that it is much more likely due to incorrect settings for the transmitter source level, athwartship steering angle and opening angle, all three of which are uniquely configured by mode (e.g. shallow vs. deep) and by ping sequence in the dual swath imaging geometry.

Though these backscatter effects can be somewhat removed in post-processing through normalization techniques, the -20dB notches of the nadir sectors is worrisome in that it might be contributing to the increased level of bottom mistracking and larger relative uncertainties of the bathymetric data in these portions of the swath (compare the backscatter bias notches of Figure 22 to the near nadir uncertainty peaks of Figure 17). Efforts were made to retrieve the configuration file to verify and correct the transmitter sector characteristics however insufficient documentation on the procedure to do so was available on the vessel at the time of the trial. It is recommended that this issue be addressed with the manufacturer to find a real-time solution that reduces the magnitude of the mean signal bias in the nadir sectors as it appears to be affecting the quality of the data over this portion of the swath.

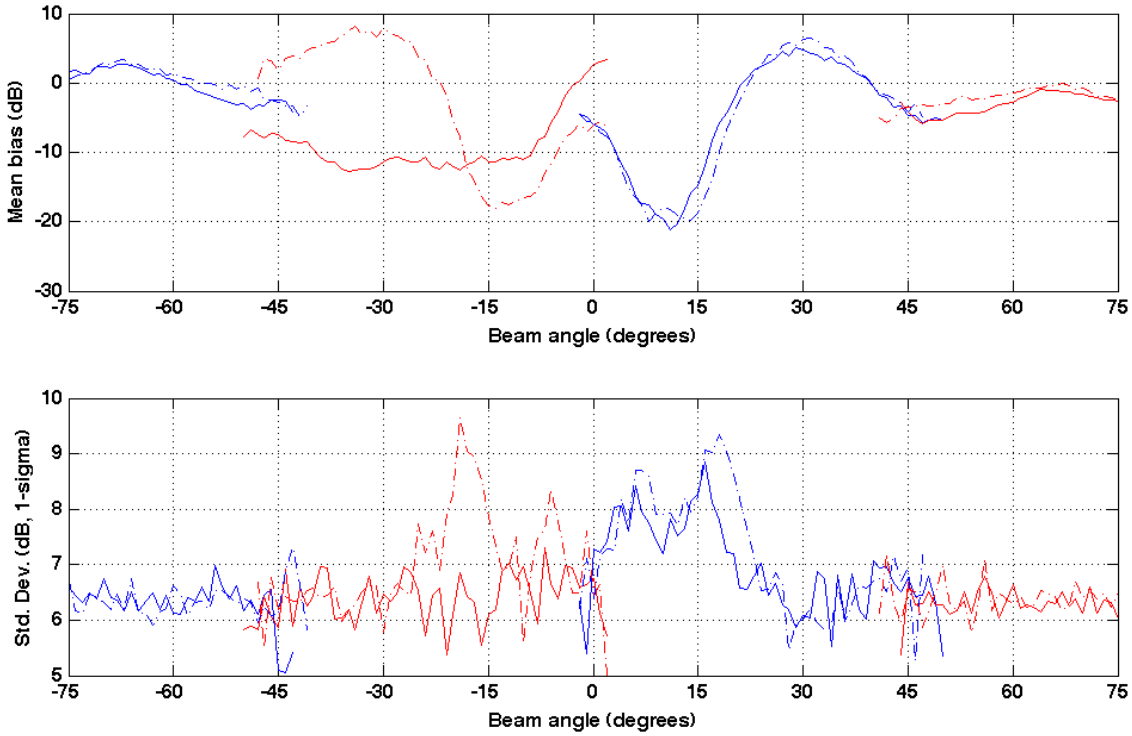

Figure 22. Beam statistics of mean backscatter bias and standard deviation by beam angle. Color coding corresponds to sector number, dashed/dotted lines correspond to ping sequence in the multi-swath ping cycle.

Puget Sound Survey (Onamac Slide)

A survey was conducted within Puget Sound in the strait immediately west of Camano Island in water depths ranging from 100m to 40m with six survey lines running N/S covering an area approximately 2300m x 8500m. In contrast to the other two surveys, no cross lines were acquired during this survey.

Despite being unable to do cross line analysis, several observations can be made regarding the performance of the mapping system in shallow, heavily sedimented inland

waterways with low seabed backscattering strength. In shallow waters, the EM302 sometimes suffers from mistracking artifacts at nadir due to penetration of the signal into the seabed and reflection off of sub-bottom layers. This can be mitigated somewhat with electronic pitch steering of the transmitter beam by a few degrees fore or aft, results may vary with differing seabed types (Gardner, 2009). This behavior was noticed several times during the transits in shallower water, especially throughout the transit leaving Puget Sound at the beginning of the trial. The transmitter array was thus intentionally steered forward for this survey resulting in tilt angles reaching up to 8º-10º. Though this was perceived to increase the bottom tracking ability during acquisition, this may have led to bottom detection biases as witnessed by the positive 1-m "hump" at nadir in the sun-illuminated topography of Figure 23. A depth cross-section is shown in Figure 24.

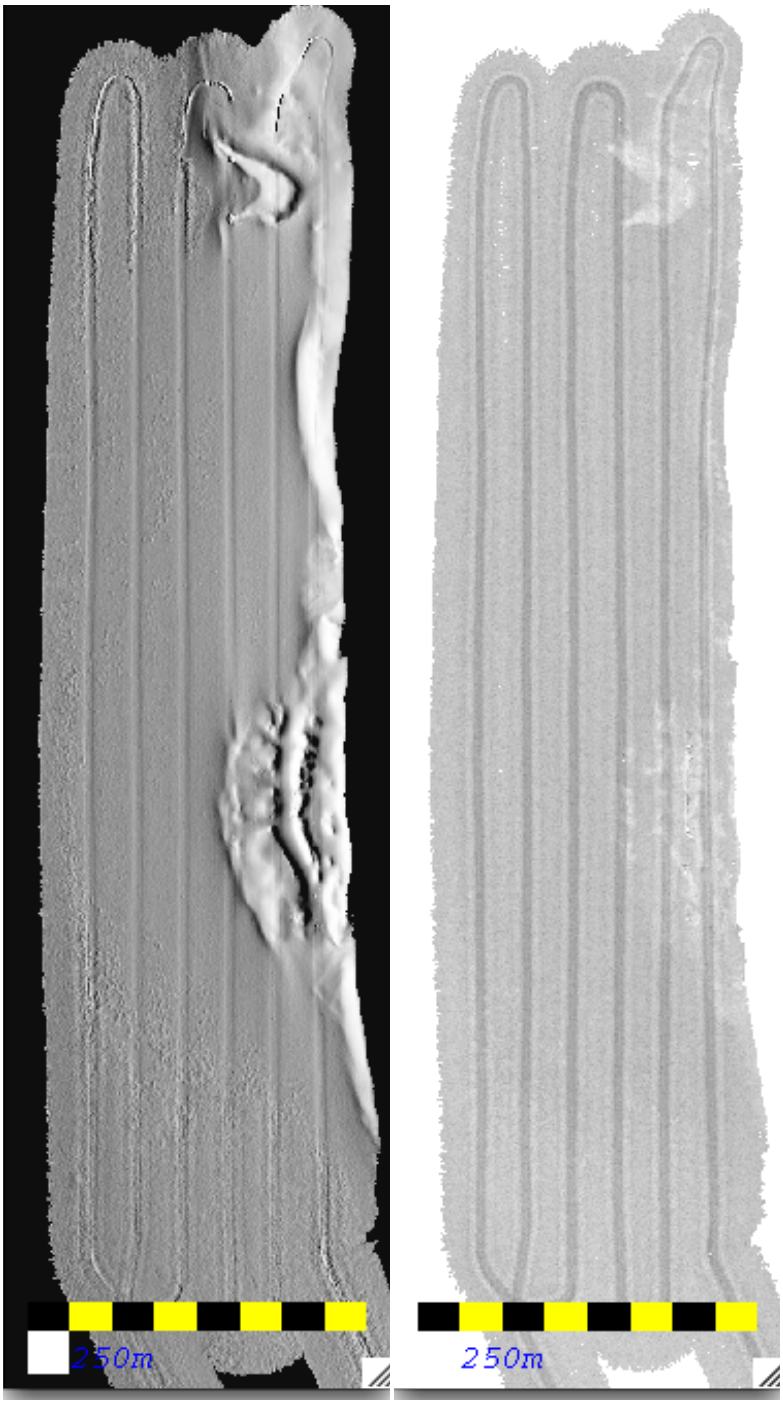

Figure 23. Sun-illuminated topography (left) and raw backscatter (right) for the Onamac Slide survey.

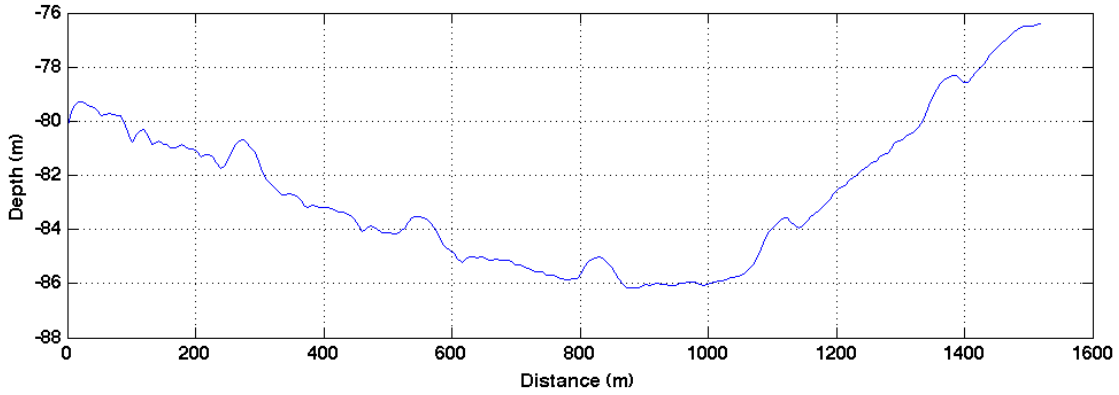

Figure 24. Sample W/E depth cross section of the Onamac Slide survey showing five passes of survey lines. Note the five ~1m amplitude "hump" artifacts associated with the nadir track of the five survey lines.

A single survey line was acquired in the normal mode of operation (i.e. no special additional transmit sector steering was applied) in Puget Sound during the return transit. This single line, in similar water depths as the Onomac Slide survey, does not exhibit the nadir hump artifact, however, it should be noted that this other area had a mean backscattering strength approximately 15dB higher than the Onomac Slide survey area. The shallow survey site, the Onomac Slide and the transit line in Puget Sound all operated in Shallow mode with dynamic dual swath and the shallow survey site and the transit line do not exhibit the artifact so the artifact does not appear related to a specific mode of operation.

The scant evidence acquired in Puget Sound alone points toward the idea that the artifact is associated with the intentional forward steering of the transmitter beams, however, the "smoking gun" is found in outbound transit data acquired in the Juan de Fuca Strait where the transmitter steering technique was first experimentally used to see if it could reduce the nadir mistracking artifacts. A survey line was found in which the setting was changed from no transmitter steering to steering on the order of 6º-7º; this run time parameter change correlates directly to the appearance of the artifact, as shown in figures 25 and 26. Figure 27 shows depth cross sections across the swath for regions before and after the application of the intentional forward transmitter steering.

In both cases, the magnitude of the hump data is consistent with the bottom detection algorithm mistracking the response from the transmitter sidelobe at nadir, e.g. for a depth of 100 m and transmit steering of 7º, the range to the seafloor at 7º should be approximately 100/cos(7º) = 100.75. Tracking the nadir transmitter sidelobe response would give a range measurement of 100, which would then reduce to a depth of 99.25m, yielding a difference of 0.75m, which is similar to the magnitude of the nadir hump artifact. This is only one potential explanation of the cause of the "hump" artifact; further testing in controlled conditions may lead to a better understanding of the cause, and more importantly, a set of optimal transmitter steering settings that help minimize the "railroad" artifact without introducing the "hump" artifact. It is recommended that effective real-time quality controls be put in place to help monitor for these types of artifacts such that preventative measures can be taken during acquisition.

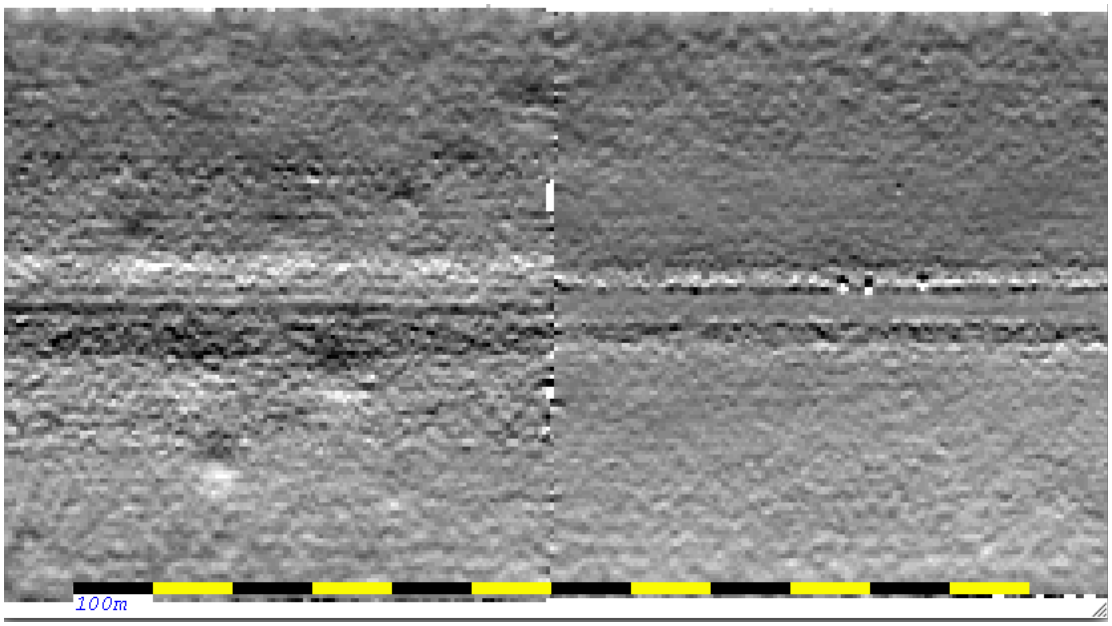

Figure 25. Sun-illuminated bathymetry highlighting the appearance of the nadir "hump" artifact associated with intentional transmitter beam steering. Vessel travel direction is right to left with the transmitter steering being applied at the midpoint in the image. Note the "railroad" artifact in the right half of the image due to mistracking on sub-bottom layers. This effect can be circumvented through steering of the transmitter beam, however, in this case one artifact is traded for another. The "railroad" artifact, however, can be filtered automatically and/or by hand without any resulting data holidays. The same cannot be said for the "hump" artifact.

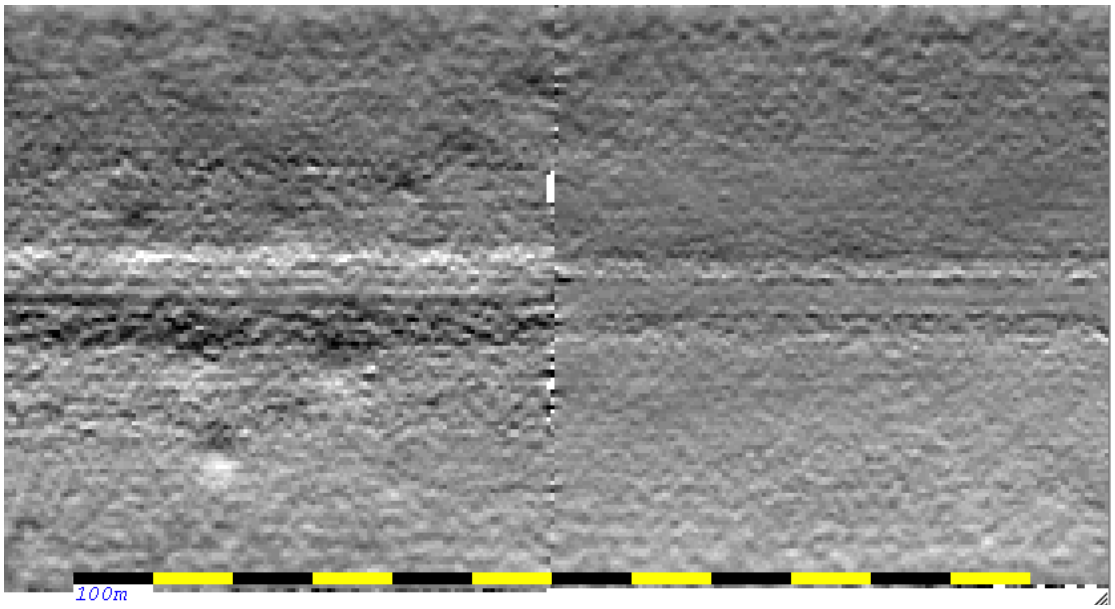

Figure 26. Same imagery as in Figure 25, however, statistical filtering has been applied to remove outliers with significantly reduced nadir "railroad" artifacts.

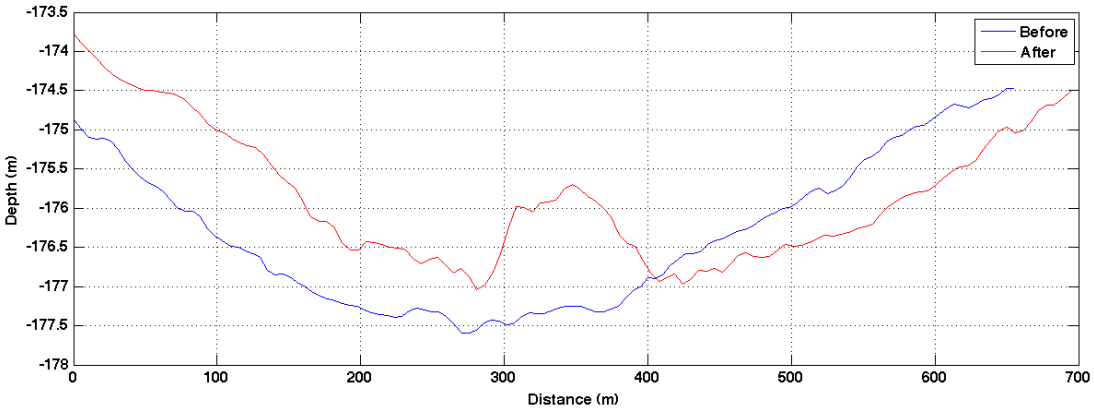

Figure 27. Depth cross sections across the swath in the region before and after application of the intentional forward transmitter steering. The "hump" artifact is approximately 1m proud of the seafloor, as was the case with the Onamac Slide survey data.

Noise Level Measurements

A series of noise level measurements were made using the EM302 BIST (built-in self test) functionality at ship speeds varying from 0-12 kts in calm sea conditions. Ten measurements of spectral and broadband noise were made at each speed and averaged to provide the plots in Figure 28-36. The noise level is more or less constant from 0kts to 8kts and increases slightly thereafter due to the vessel requiring additional generators to travel at speeds higher than 8kts. The general trend of the spectral noise levels is consistent over most speeds with a band wide increase in the noise level at speeds of 10-12kts. Lower frequencies experience higher noise levels, this could be associated with some of the sector specific noise that was observed intermittently throughout the trial in the real-time water column imagery display of the EM302 operation station. It is interesting to note that the overall noise does not increase significantly when adding an additional engine, see figures 33 and 34 specifically.

It has been noted throughout the entire SAT trial that other acoustic systems onboard the vessel occasionally interfere with the EM302 operation. It is our understanding that a synchronization unit will be installed in the near future; this system should remove the few interference problems that have been observed to date. For the time being, a simple external trigger has been installed that allows the EM302 to control the ping interval of the Knudsen 3.5kHz sub-bottom profiler. Without these precautionary measures, it may not be possible to acquire EM302 (30kHz) and Knudsen (3.5kHz) data simultaneously without some level of interference in the EM302 data.

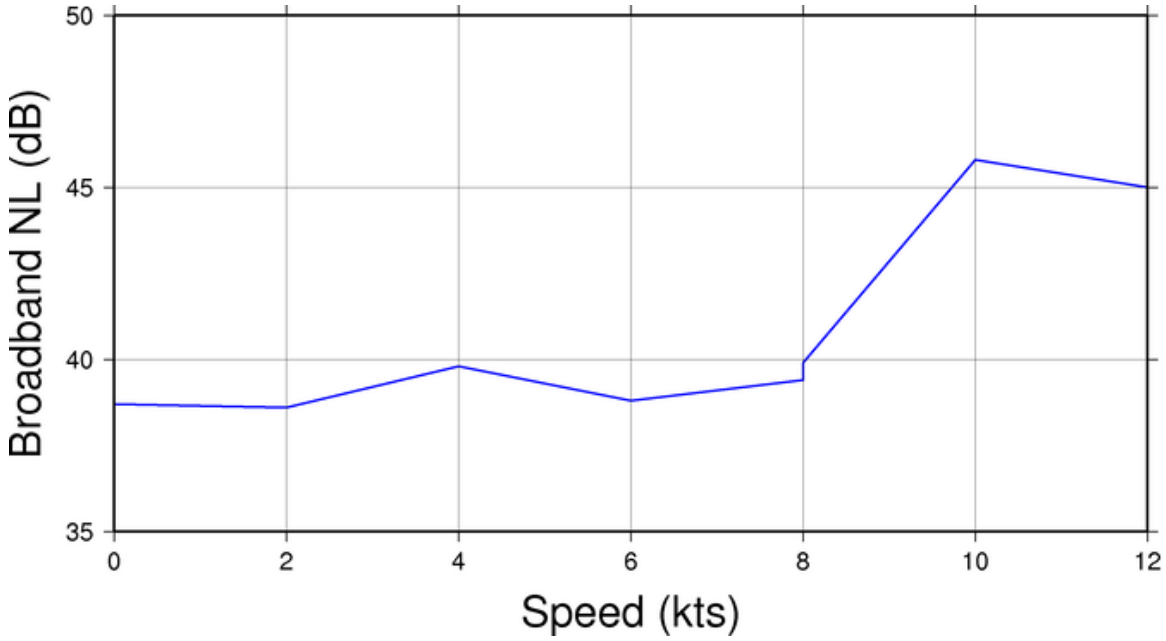

Figure 28. Broadband noise levels versus ship speed.

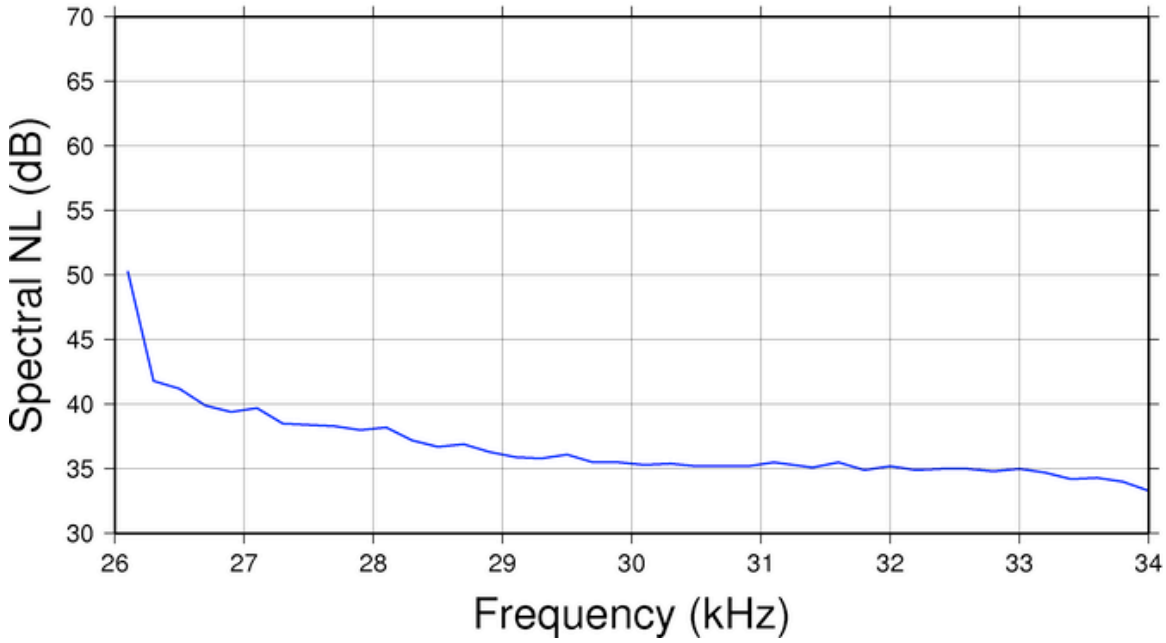

Figure 29. Noise spectrum at 0kts/0rpm.

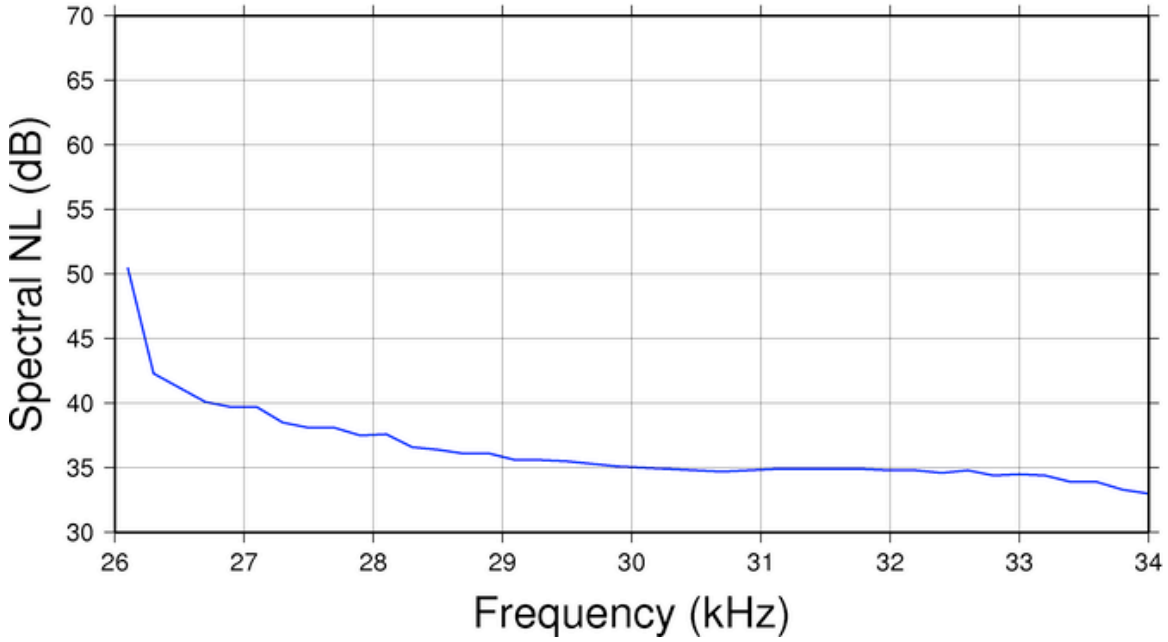

Figure 30. Noise spectrum at 2kts/23rpm.

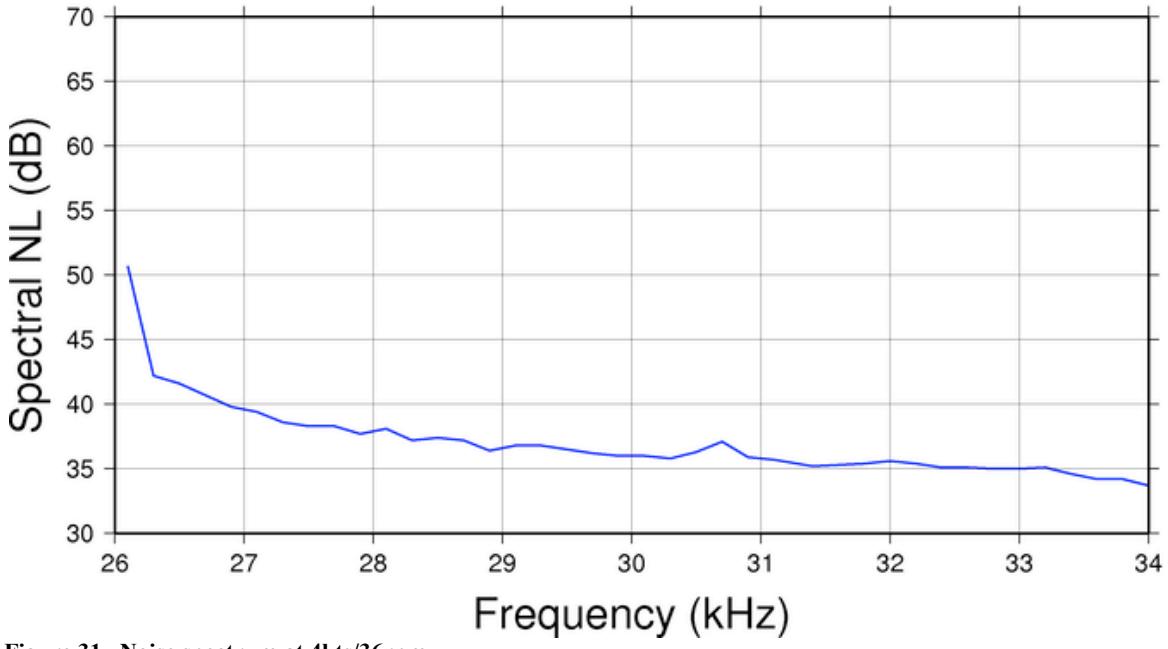

Figure 31. Noise spectrum at 4kts/36rpm.

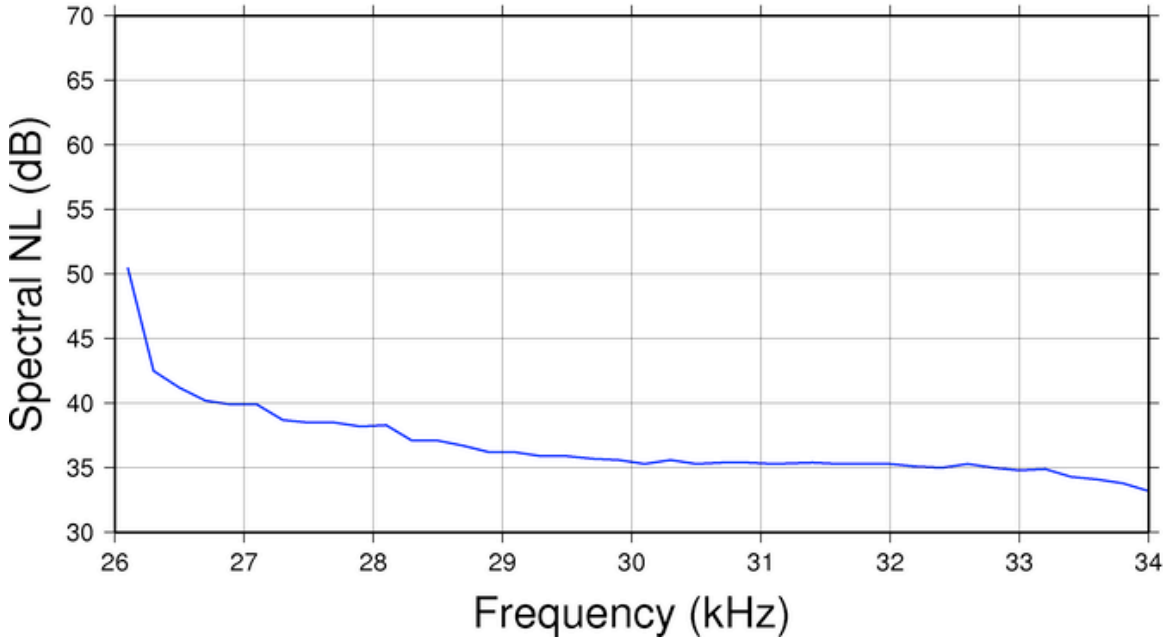

Figure 32. Noise spectrum at 6kts/53rpm.

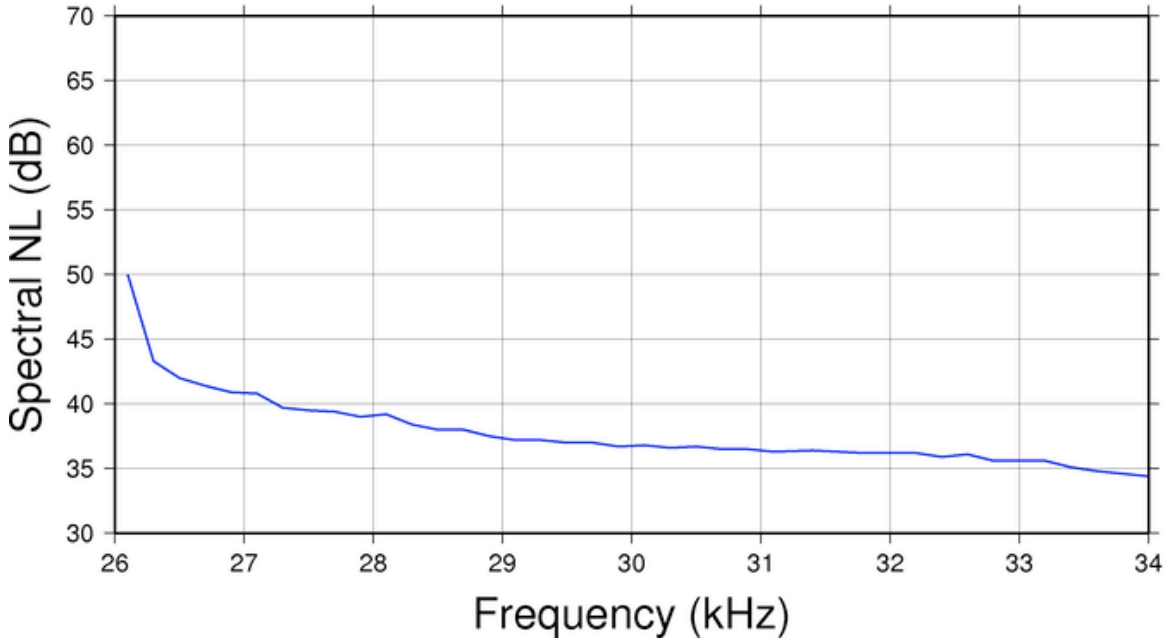

Figure 33. Noise spectrum at 8kts/71rpm.

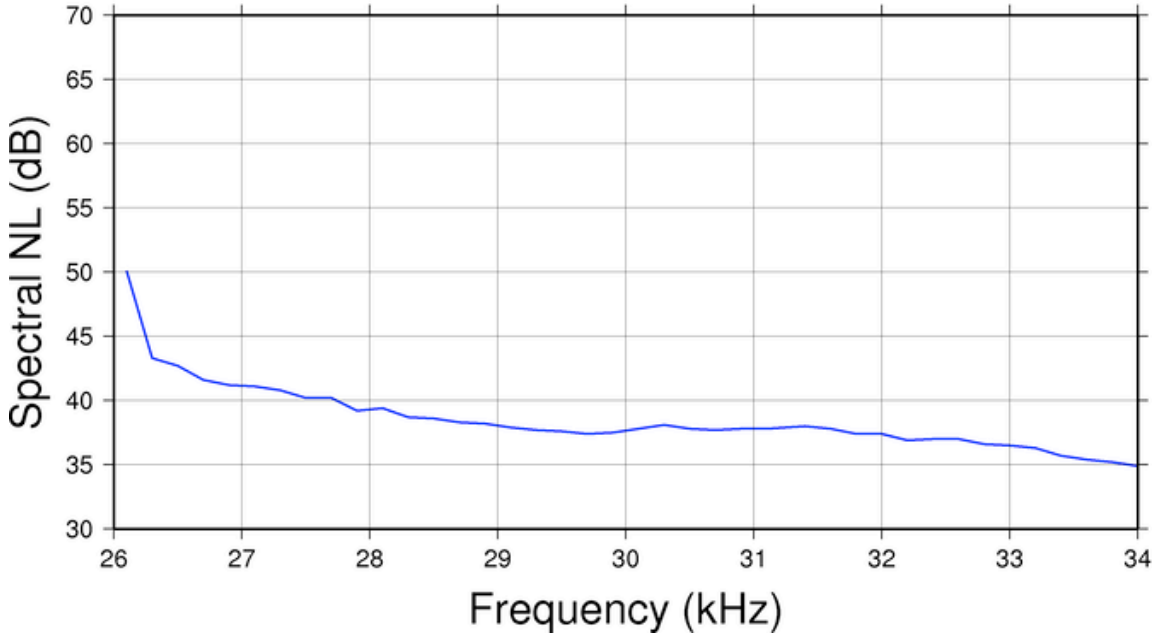

Figure 34. Noise spectrum at 8kts/71rpm with 2 engines.

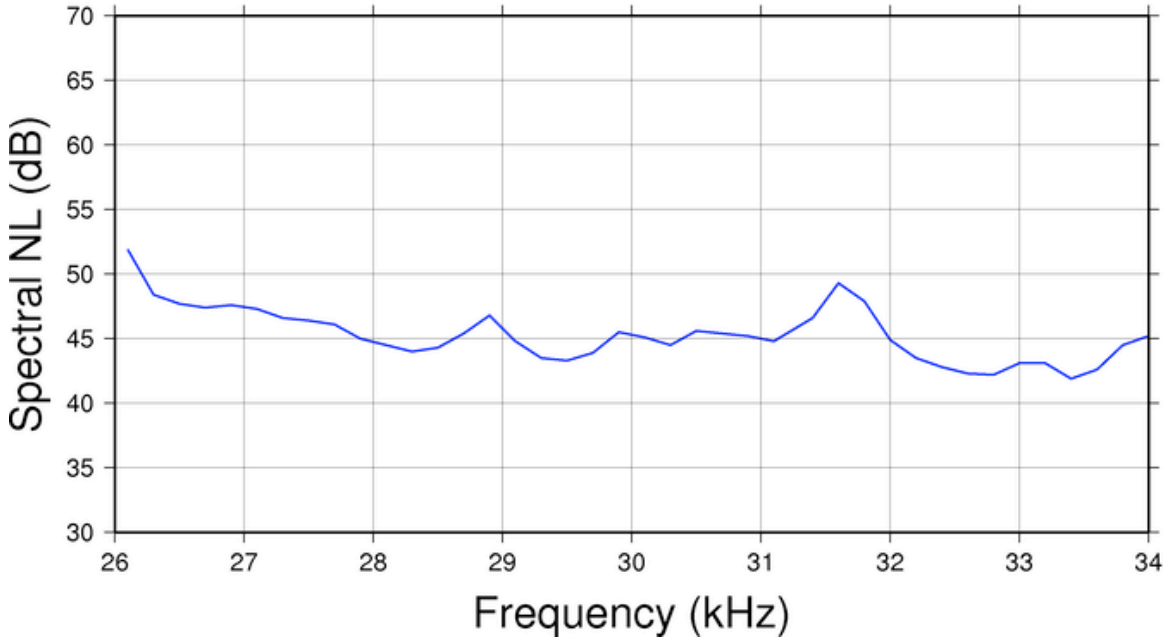

Figure 35. Noise spectrum at 10kts/88rpm with 2 engines.

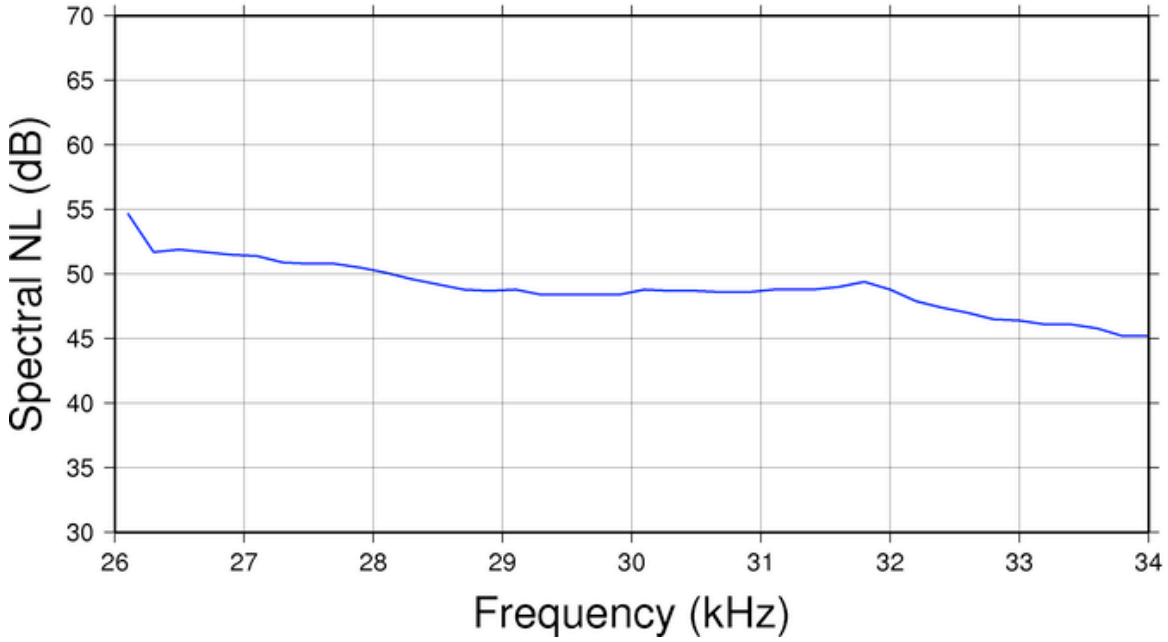

Figure 36. Noise spectrum at 12kts/112rpm with 2 engines.

EM302 data were acquired at the same speeds in Deep mode with the angular sector open to +/-75º. Results are presented below in a sun-illuminated bathymetry map of a 25kmx30km region; number labeling corresponds to ship speed in knots (Figure 37). Note that the bathymetric noise level and coverage do not appear to vary dramatically over the range of speeds in the test.

After the noise level tests, EM302 data were acquired in 1000-1700m of water, a subset is shown in the sun-illuminated image of Figure 38 which depicts an area covering roughly 30km by 30km. Data in the image were gridded without any manual or automated data filtering, i.e. these are the raw data. There is no evidence of degradation of swath coverage over the course of the line and the number of outlier bottom detections is small indicating that the system is having little difficulty in tracking the seafloor at a speed of 12kts. Small (1-2m) ribbing type artifacts are apparent in the outermost sector and represent a small source of uncertainty (0.1%w.d.); these are noticeable due to the nearest neighbor gridding algorithm that was used and they would not be visible if a more appropriate gridding algorithm was used that allowed for the radius of influence of each beam to capture more than the nearest grid node (e.g. inverse distance weighting with a projected beam footprint radius of influence).

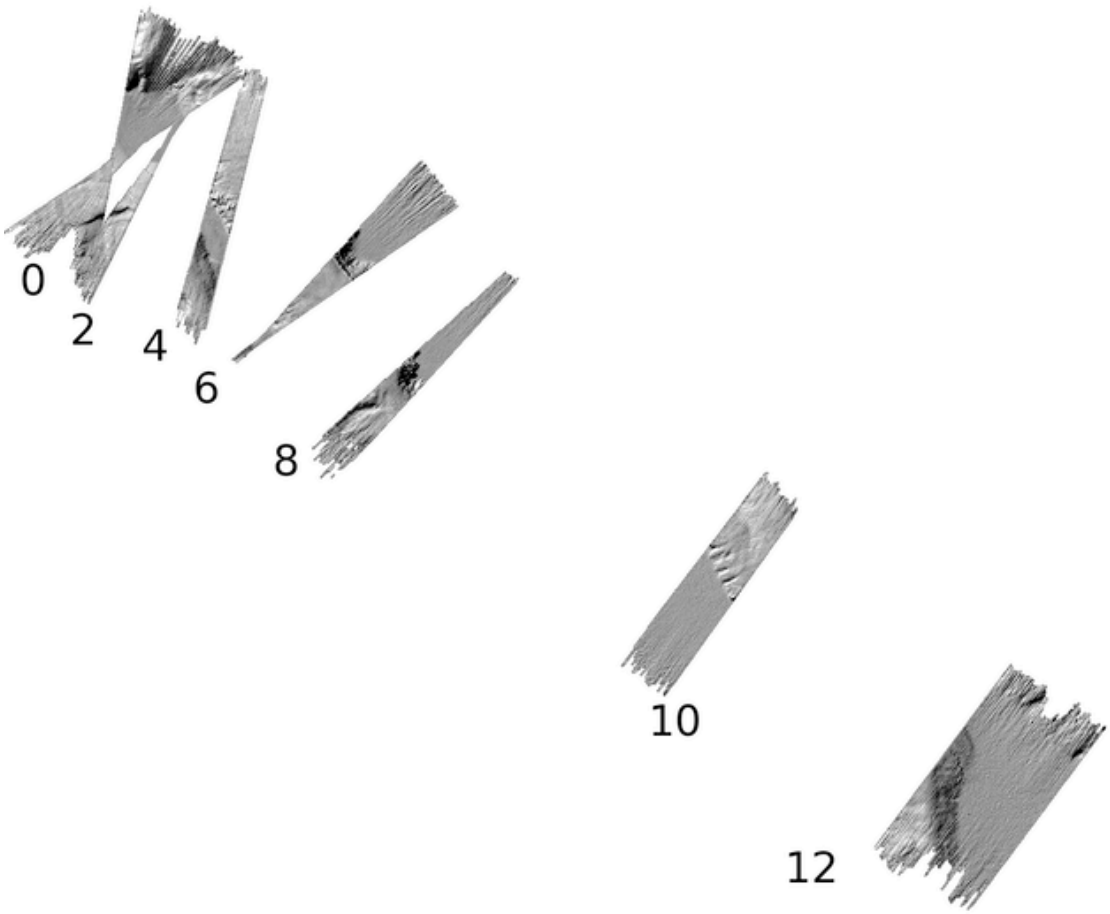

Figure 37. EM302 data acquired at various ship speeds between noise level tests. Numeric labeling indicates ship speed in knots.

The overall ship noise level is low and should not be an issue for most mapping operations as the vessel typically works at survey speeds less than 10kts. This operating procedure may change given that the EM302's dual swath option allows for increased survey speeds without loss of along track sounding density. Given the results seen in this test, it appears that the vessel can effectively acquire clean bathymetric data at speeds of 12kts.

It should be noted that it was not possible to test the system coverage performance in deep water with higher sea states; future survey projects in higher sea states can be used to collect baseline statistics of the system's mapping capability in higher sea states to provide guidance for achievable swath widths under higher noise levels.

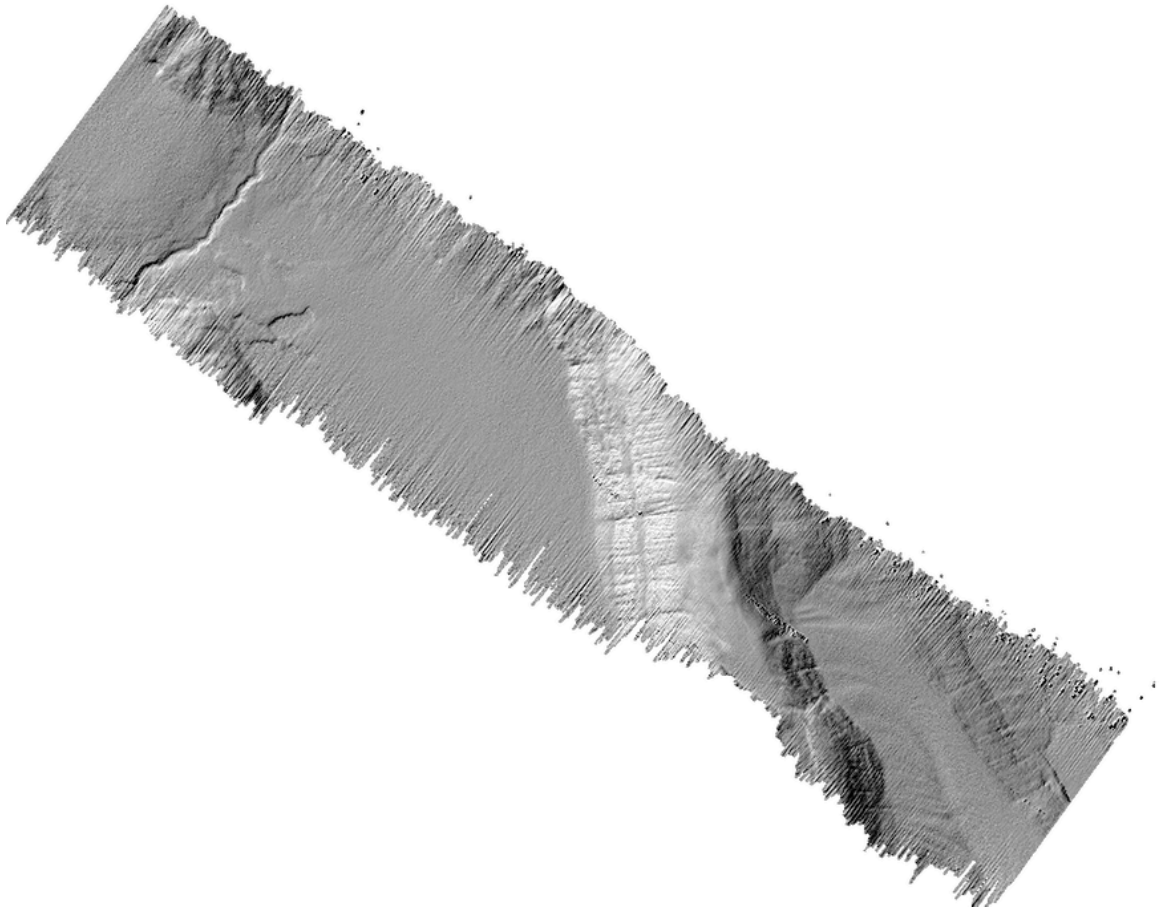

Figure 38. EM302 data acquired at 12knots during transit after the noise level tests. Bathymetric noise levels are slightly higher in the outermost sector, deviating approximately 1-2m from the mean.

Conclusion and Recommendations

The results of this analysis indicate that the EM302 was functioning, for the most part, as expected with all results indicating that the integration of all sensors was done correctly. Bathymetric repeatability and accuracy was within expected levels for both deep water and shallow water with minor mistracking issues that can likely be easily remedied through additional efforts to verify and correct the transmit sector geometry and optimize the forward steering of the transmit fan to minimize nadir mistracking without introducing the so-called "hump" artifact.

Backscatter data were acquired and analyzed in both deep and shallow areas. Deep water performance was acceptable with minor beam pattern type artifacts that were easily removed through standard normalization techniques. Performance in shallow water (in shallow mode) was less than acceptable with significant beam pattern type artifacts in the transmit sectors immediately adjacent to the nadir region, this was further compounded by the large discrepancy between transmit sector beam patterns between the pings in dual swath mode on the port side. As with the nadir mistracking, it is expected that these

issues can be mitigated through verification and correction of the transmit sector configuration file.

Several recommendations can be made based on observations made during the trial and afterwards during the analysis of the data:

- Focused testing should be done in a controlled environment with the cooperation of Kongsberg technicians to improve the transmit sector configuration in shallower water in addition to finding optimal settings to mitigate nadir mistracking in shallow waters without introducing the “hump” artifact.
- The auxiliary GPS offsets in the POSMV be set to zero to avoid future confusion.
- The water line position with respect to the reference point should be confirmed with dockside observations and verified against the value currently being used by the EM302.
- Add GB Networking switch throughout labs and particularly to each center table in the main lab.
- Add large format LCD screen as extended desktop to SIS computer. This could be mounted on a manufactured "fence" behind the SIS station such that the secondary screen is hung above the current screen.
- Get rid of wheels on all chairs.
- Post computers, IP addresses and shared directories for commonly used systems so scientists can easily find them.
- Large whiteboard in the main science lab.
- Need a real-time display of ship's position on a map in main science lab. Ideally this would also display waypoints and other ancillary data added by the science party.
- Post messages broadcast by UDP on the ship's network and the ports where they can be found.
- Provide permanent workstations for MB data processing.

References

Gardner, J.V., Malik, M.A., 2009, "U.S. Law of the Sea Cruise to Map the Eastern Mendocino Ridge, Eastern Pacific Ocean", University of New Hampshire (UNH), Center for Coastal and Ocean Mapping (CCOM)/Joint Hydrographic Center (JHC), Durham, NH, 34 pages. Report.

Hamilton, T. and J. Beaudoin, 2010, "Modeling Uncertainty Caused by Internal Waves on the Accuracy of MBES", International Hydrographic Review, No. 4, pp. 55 - 65. Journal Article.

Moum, J. N., D. M. Farmer, W. D. Smyth, L. Armi, S. Vagle, 2003. “Structure and Generation of Turbulence at Interfaces Strained by Internal Solitary Waves Propagating Shoreward over the Continental Shelf”, J. Phys. Oceanogr., No. 33, pp. 2093–2112.